

Topological active matter

Suraj Shankar,¹ Anton Souslov,² Mark J. Bowick,³ M. Cristina Marchetti,⁴ and Vincenzo Vitelli^{5,6,7}

¹*Department of Physics, Harvard University, Cambridge, MA 02318, USA*

²*Department of Physics, University of Bath, Claverton Down, Bath BA2 7AY, UK*

³*Kavli Institute of Theoretical Physics, University of California Santa Barbara, Santa Barbara, CA 93106*

⁴*Department of Physics, University of California Santa Barbara, Santa Barbara, CA 93106, USA*

⁵*James Franck Institute, The University of Chicago, Chicago, IL 60637, USA*

⁶*Department of Physics, The University of Chicago, Chicago, IL 60637, USA*

⁷*Kadanoff Center for Theoretical Physics, The University of Chicago, Chicago, IL 60637, USA*

(Dated: July 20, 2021)

Active matter encompasses different nonequilibrium systems in which individual constituents convert energy into non-conservative forces or motion at the microscale. This review provides an elementary introduction to the role of topology in active matter through experimentally relevant examples. Here, the focus lies on topological defects and topologically protected edge modes with an emphasis on the distinctive properties they acquire in active media. These paradigmatic examples represent two physically distinct classes of phenomena whose robustness can be traced to a common mathematical origin: the presence of topological invariants. These invariants are typically integer numbers that cannot be changed by continuous deformations of the relevant order parameters or physical parameters of the underlying medium. We first explain the mechanisms whereby topological defects self propel and proliferate in active nematics, leading to collective states which can be manipulated by geometry and patterning. Possible implications for active microfluidics and biological tissues are presented. We then illustrate how the propagation of waves in active fluids and solids is affected by the presence of topological invariants characterizing their dispersion relations. We discuss the relevance of these ideas for the design of robotic metamaterials and the properties of active granular and colloidal systems. Open theoretical and experimental challenges are presented as future research prospects.

Active media are out-of-equilibrium systems composed of individual components that convert energy into non-conservative forces and motion at the microscale [1–3]. Examples include self-propelled particles (e.g., micron-sized colloids powered by chemical reactions) [4, 5], biofilaments with molecular motors [6, 7] and many biological systems ranging from epithelial tissues and bacterial colonies to bird flocks [8–10]. Describing these media using continuum equations, as you would for passive fluids or solids, requires a careful re-examination of the symmetries and conservation laws that are present (or absent!) in each active system [2]. The most obvious example is the conservation of energy, which is manifestly violated by the presence of molecular motors or other mechanisms of energy transduction at the microscale that power self-sustained flows and active stresses. The energy injected at the microscale is responsible for morphological features and transport properties absent at equilibrium that are robust against certain perturbations. Some of these robust features can be analyzed using a branch of mathematics called topology.

Topology describes properties of objects that are preserved under continuous deformations of their shapes. A common example is the smooth deformation of a doughnut into a mug (with a handle). During this transformation, the shape of the object changes but the number of handles, ν —seen as holes from a three-dimensional viewpoint—is preserved, as long as no tear is generated. The integer ν , called the genus, is an example of a topological invariant. In condensed matter physics, a prime application of topological invariants is in the char-

acterization of topological defects, which are particle-like objects that describe global deformations of an ordered medium [11–13]. As an example, consider a vortex (Box 1) in a two-dimensional (2D) vector field that represents, for instance, the local orientation of elongated molecules lying in the plane. While the location of an isolated vortex can be parameterized by the position of its center, its presence disrupts molecular alignment throughout space.

The global character of a vortex is captured mathematically by the definition of its winding number. Start by introducing the field $\theta(\mathbf{r})$ that describes the local angle that the molecules (i.e., the vector order parameter) make with respect to a fixed direction in the plane. The winding number, ν , is then an integer that tracks the cumulative change in $\theta(\mathbf{r})$ along *any* path enclosing the vortex:

$$\nu = \frac{1}{2\pi} \oint \nabla \theta \cdot d\mathbf{l}. \quad (1)$$

Very much like the number of handles on a surface is preserved under continuous deformations of its shape, the integer ν is also a topological invariant. The only difference is that in this case, ν is preserved under continuous deformations of the vector order parameter. As a result, a vortex characterized by the non-vanishing winding number $\nu = 1$ is said to be topologically stable or robust: it cannot be made to disappear ($\nu \rightarrow 0$) unless annihilated with a topological defect characterized by a winding number of opposite sign, i.e., an anti-vortex (Box 1). Note that if the line integral in Eq. (1) is evaluated along a path

encircling multiple vortices and anti-vortices, ν measures the *net* number of topological defects (to which a positive or negative sign is assigned depending on their individual winding numbers).

A similar mathematical mechanism ensures the robustness of so-called chiral edge modes in topological insulators [14–17]. A defining feature of these wave modes is that they propagate unidirectionally along sample boundaries without experiencing any backscattering even if they encounter sharp corners or obstacles on their way [18, 19]. This property can be traced to the presence of a topological invariant called a Chern number [20]. This integer, that we once again denote by ν to emphasize the analogy with the previous case, measures the *net* number of unidirectional, i.e., chiral, edge modes present (to which a positive or negative sign is assigned depending on whether the modes propagate clockwise or counterclockwise). These modes are said to be topologically robust, much like the vortices discussed above. In this case, the Chern number (and hence the very presence of an edge mode) is preserved under continuous changes in the *physical* parameters of the material (rather than under continuous deformations of the *order* parameter). On a more technical level, we shall see that topological invariants, such as Chern numbers, can also be viewed as winding numbers encircling topological defects, but in *wave-vector* space.

Topological defects and topological protected modes are intertwined [21–24]. In addition to boundaries, topological modes can be localized around defects such as vortices, dislocations or domain walls. Topological defects [11, 13, 25] and topologically protected modes [26–31] occur in a variety of physical contexts, but in active media they acquire distinctive properties, which are the focus of this review.

Since active media display non-conservative stresses and spontaneous flows, they naturally break key symmetries that passive materials would possess [2, 3]. For example, active media can violate reciprocity [32, 33], defined as the symmetry between perturbation and response, as well as detailed balance [34, 35], defined as the symmetry between the past and the future within the dynamics of microscopic processes. Non-equilibrium violations of either of these principles introduces an arrow of time and enables the presence of non-vanishing currents (of energy, momentum, or particles) in the steady state of active systems. In turn, these currents endow topological modes and defects with properties absent at equilibrium and, in some cases, enable their very existence. In order to illustrate this point, consider the following two examples.

First, topological defects (which normally cost a large elastic energy [25]) can unbind and proliferate even at zero temperature if active stresses are present [36, 37]. This unbinding occurs in active nematics [38, 39], which are liquid-crystalline media composed, for instance, of cytoskeletal filaments driven by molecular motors [7, 40]. Moreover, the resulting topological defects can move by

themselves, i.e., even in the absence of external forces or fields [7, 41, 42]. This spontaneous “self-propulsion” depends on the winding number of the defects [42] and ultimately originates from the presence of non-conservative internal forces generated by ATP-powered molecular motors on the microscale.

Second, chiral edge modes occur in mechanical, optical, and electronic systems [15, 26–31], but in the simplest situation, external (e.g., magnetic) fields are typically required to break the symmetry between left and right-moving waves. A simple way to break this symmetry in mechanics is to build a lattice of circulators [43, 44]. A circulator is a ring in which air is constantly moved by a fan, for example clockwise. Experiments [43, 44] reveal that when many such circulators are assembled into a lattice, the sound waves propagating on top of the flowing fluid are topologically protected. If one now fills the rings with self-propelled particles (instead of a passive fluid like air), the required flow arises spontaneously without motorizing the circulators: the microscopic particles themselves are motorized [45]!

In the remainder of this review, we build on the examples considered above and provide an introduction to the theory of topological active matter as well as a survey of its rich experimental ramifications.

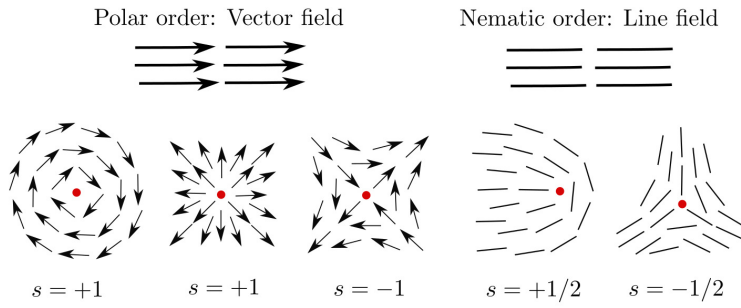
I. TOPOLOGICAL DEFECTS IN ACTIVE MATTER

In passive materials, topological defects are inevitably formed in quenches from the disordered into the ordered state or when order is frustrated by curvature, external fields, or boundary conditions. They constitute elementary excitations of the homogeneous ordered state and their statistical mechanics offers a picture dual to that of the familiar order parameter [13]. Order-disorder transitions in many passive two-dimensional systems, including superfluid and superconducting films, crystalline layers and 2D nematics, are controlled by the unbinding of topological defects through the celebrated Berezinskii-Kosterlitz-Thouless mechanism (BKT) [46–50]. The BKT theory reveals a distinctive universality class of defect-induced continuous phase transitions at equilibrium [50]. The theory relies on the mapping of the statistical physics of point defects onto a gas of interacting Coulomb charges. At low temperature, opposite-sign defect pairs are bound by Coulomb-like attraction and the state remains ordered. Above a critical temperature, entropic effects overcome energetic attraction resulting in defect unbinding, which destroys the ordered state [13, 25].

Just as in equilibrium, defects play an important role in the spatiotemporal dynamics and relaxation of *active* ordered phases. We focus here on orientationally ordered fluids which can host point-like defects in two dimensions (2D), and both point- (monopoles, also called asters) and line-like defects (disclinations) in three dimensions

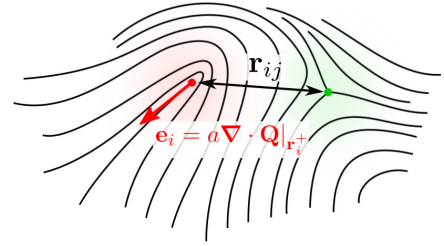
Box 1: Topological defects in passive and active ordered fluids.

Topological defects are special zeros of the order parameter field. They are point-like in 2D liquid-crystalline media and are classified by their winding number or topological charge $s = \Delta\Theta/2\pi$ (also see Eq. 1), where $\Delta\Theta$ is the net angle through which the order parameter rotates as one encircles the defect. The charge s is positive if the order parameter rotates in the same direction as the path traversed, negative if it rotates in the opposite direction. In a 2D XY magnet where the order parameter is a vector field, the lowest charge topological defects are asters and vortices (both with $s = +1$), and anti-vortices or cross-hairs (with $s = -1$). In a nematic film, where the broken symmetry identifies only orientation (not direction) and the order parameter is a line field, the lowest energy defects are disclinations of strength $s = \pm 1/2$.

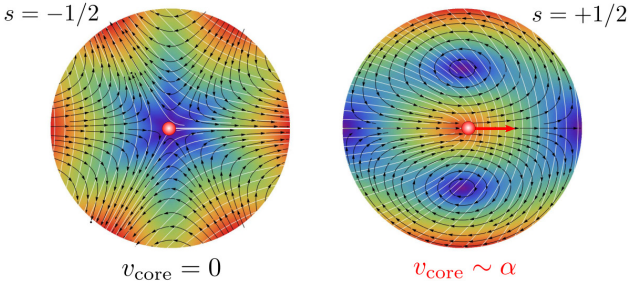


In 2D passive liquid crystals, two defects of strength s_i and s_j and separation \mathbf{r}_{ij} interact via a Coulomb potential, mediated by nematic elasticity (K) and cutoff by the defect core size (a).

$$V(\mathbf{r}_{ij}) = 2\pi K s_i s_j \ln\left(\frac{|\mathbf{r}_{ij}|}{a}\right)$$

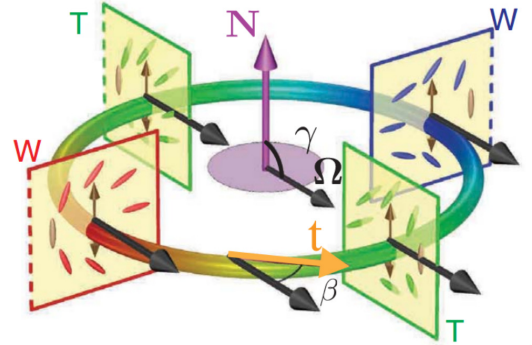


In 2D *active* nematics, defects behave like quasiparticles “dressed” by the active flows they produce [36,39,42]. Such a description is appropriate deep in the nematic regime, where the defect core size (a) is the smallest length scale in the system. The flow generated by a $+1/2$ defect is finite at the core, rendering the defect a self-propelled particle with a well-defined polarization (\mathbf{e}_i). On the other hand, the flow generated by a $-1/2$ defect vanishes at the core. To leading order in activity, defects interact via the same Coulomb force as in the passive case but also exert active torques on each other. Defects in active nematics therefore behave as an interacting mixture of active ($+1/2$) and passive ($-1/2$) charged quasiparticles [36].



The flow \mathbf{u} generated by a defect extends through all space and is obtained by solving the Stokes equation that balances active stresses of strength α due to a defect texture described by the nematic order parameter \mathbf{Q} with frictional and viscous damping [42,81] (also see Box 2).

Bulk active nematics support topologically neutral disclination loops that smoothly interpolate $+1/2$ and $-1/2$ defect textures in local cross-sections of the loop. The $\pm 1/2$ wedges are equivalent in 3D by escape into the third dimension. The simplest of such wedge-twist loops is characterized by a rotation vector ($\boldsymbol{\Omega}$) in the plane of the loop ($\gamma = \pi/2$), making an angle β with the local tangent (\mathbf{t}). Similar to their 2D counterparts, the local active flows generated by such disclination loops drive complex dynamics in 3D bulk active nematics [87].



(3D) [11, 12]. Collections of polar active particles with aligning interactions, akin to “flying spins,” can order in states of collective motion where the order parameter is the mean velocity of the flock (see Box 2). In these *polar* active fluids, also called Toner-Tu fluids [51–54], the ordered state is a state of mean motion that spontaneously breaks rotational symmetry and time-reversal symmetry (TRS) on a global scale. In contrast, active

nematics [38, 39] are composed of head-tail symmetric rod-like entities that exert internally generated stresses on their surroundings and organize in states of *apolar* orientational order. These fluids display no net motion on average, but combine the rich rheology of liquid crystals with active driving. Box 2 describes some commonly used continuum models to describe such systems.

Active ordered fluids have been assembled from a va-

riety of soft materials [5–7, 55, 56]. The orientationally ordered state becomes unstable on length scales L when active stresses of order $|\alpha|$ (see Box 2) exceed elastic stresses $\sim K/L^2$ [57], with K the liquid-crystalline stiffness. Bulk ordered states ($L \rightarrow \infty$) are therefore unstable for any amount of activity, but can be stabilized by confinement [58] as well as by friction with a substrate [59] below a critical value of activity. At large activity, all liquid-crystalline active fluids display turbulent-like dynamics with a proliferation of topological defects. Polar fluids with vectorial order parameters exhibit defects such as vortices and asters characterized by an integer topological charge. In contrast, the inversion symmetry of nematic order means that the order parameter maps onto itself after a winding of only 180° around the defect core—the small, roughly circular, region of space of radius a surrounding the defect center where the nematic order parameter vanishes. This allows defects with half-integer charge known as disclinations (see Box 2). Since the energetic cost of a defect is proportional to the square of its charge, $\pm 1/2$ disclinations are the lowest energy defects in nematics; they are not allowed in polar (vector) fluids. The presence of $\pm 1/2$ defects therefore provides a fingerprint of the apolar nature of the broken symmetry and a criterion for distinguishing nematic from polar order.

Asters and vortices have been observed in high-density motility assays [60, 61], confined and membrane-bound reconstituted cortical extracts [55, 56, 62], and suspensions of colloidal rollers motorized by an electric field [63]. Nematic disclinations have been identified in diverse systems, including cytoskeletal filament-based active nematic suspensions [7, 40, 64, 65], collections of living cells [66–72], and even multicellular organisms [73]. In recent years topological defects have been the focus of intense research, particularly in active nematics [39], which exhibit self-sustained and spatiotemporally chaotic large-scale flows accompanied by the spontaneous proliferation of topological defects. It is then natural to ask if the chaotic dynamical state of active nematics can be understood from the perspective of defect unbinding, and if the equilibrium BKT transition has an analogue in the active realm.

In both passive and active liquid crystals, distortions of orientational order generate flows, and flows in turn deform the ordered state. The key distinction between passive and active systems is that in the former, flows and deformations are generated by applying external fields or via boundary conditions. Such flows are transient: the system always relaxes to the equilibrium (ordered) state upon removal of perturbations or constraints. In active systems, in contrast, flows and deformations are internally generated and self-sustained. In 2D, bulk active nematics are generically unstable to bend or splay deformations generated by local active fluctuations [57]. As these distortions grow in time, they generate flows that further enhance the deformations, ultimately generating unbound pairs of topological defects. Such spon-

taneously generated defects are themselves strong distortions of orientational order and yield distinctive flow patterns [42, 74]. This intimate connection between defects and flows, offers the opportunity to direct and localize nonlinear active flows by controlling the dynamics of topological defects [37, 75, 76]. Recent work has even suggested that biological systems may exploit this connection between structure and dynamics and use defects to localize stresses and perform specific biological functions [71–73, 77–80]. These subjects will be the focus of the rest of this section.

A. Active defects spontaneously move

One of the distinguishing aspects of defects in active matter is their capacity for spontaneous and autonomous motion. The large distortions of the order parameter around a topological defect generate local active flows, whose symmetry and profile is controlled by the defect geometry. In particular, in 2D active nematics, the comet-like $+1/2$ defect (see Box 1) generates a flow that is finite at the defect core. The $+1/2$ defect then rides along with the flow it generates, behaving like a self-propelled polar particle [42, 81]. In contrast, the flow generated by a $-1/2$ defect vanishes at the defect core due to the defect’s threefold symmetry (see Box 1), and to leading order in activity this defect remains a “passive” particle. The direction of motion of the $+1/2$ defect is determined by its local orientation or polarity and by the sign of the active forcing. Active stresses that cause material extension along the ordering axis are called “extensile,” while those that contract along the same axis are called “contractile.” In extensile fluids, $+1/2$ defects actively propel themselves along the head of the comet, while in contractile systems the active propulsion is directed along the comet’s tail. If chiral active stresses are present, $+1/2$ disclinations self-propel instead at an angle relative to their polarity [82, 83], and intrinsic active spinning renders defect trajectories circular [82]. In polar fluids, charge $+1$ spiral vortices undergo spontaneous rotation [84] due to the chirality of their spiral texture. Other low charge defects, such as circularly symmetric asters and antivortices, perform neither rotational nor translational spontaneous motion. In contrast to defect motion in externally driven systems, the motion of active defects is dictated by the local *geometry* of the defect itself and not by a fixed external field, as would be the case, for example, for driven vortices in a superconducting film. This profound distinction leads to a plethora of phenomena characteristic of active matter.

Defects can also occur in 3D active suspensions, but they are less well understood. As in 2D, bulk active nematics in 3D are susceptible to a generic hydrodynamic instability [57] that spontaneously generates individual charge-neutral disclination loops [85–88] (see Box 1). Unlike in 2D, where topological charge conservation constrains point defects to be created and annihilated in

pairs of opposite charge, in 3D *charge-neutral* disclination loops [12] can be nucleated on their own. The active flows caused by the director distortion around such a disclination loop cause it to stretch, twist, and buckle [88]. The complex configurational dynamics of these loops combined with topological reconnections leads to chaotic 3D flows which, recently, have been observed in simulations [85, 86] and experiments [87]. Recent theoretical work has also extended similar ideas to chiral phases such as bulk active cholesterics [89–91]. Here, λ -lines, which are defects in the cholesteric pitch with no director singularity at their core [89] and other nonsingular topological textures called half-skyrmions or merons [90] can sustain coherent rotations and steady defect patterns along with spatiotemporal chaotic flows, even though these defects are not self-propelled.

B. Defect dynamics, unbinding, and ordering out of equilibrium

From a fundamental point of view, defect motility raises intriguing possibilities for phase transitions. The consequences of defect self-propulsion have been explored predominantly in 2D active nematics [36, 37, 42, 74, 81, 94]. The defect-driven chaotic flows lead to a state dubbed “active turbulence” [74, 95], which is characterized by vorticity and shear flows on a typical length scale that controls the mean defect separation and is set by a balance of active and elastic stresses [68, 74, 96–98]. The phenomenology and scaling properties of active turbulence have been detailed in recent reviews [39, 99]. Here we focus on its topological aspects and sketch the physical arguments underpinning the unbinding of active defects [36].

At equilibrium, defects in 2D behave as point charges that interact via a Coulomb potential. This pair interaction is mediated by the underlying elasticity of the ordered fluid and scales as $K \ln(r/a)$, where K is an elastic stiffness, r is the pair separation and a the defect core size (see Box 2). In a 2D *active* nematic, an isolated $\pm 1/2$ disclination pair continues to experience the passive attractive force $\sim K/r$ from elasticity, but in addition, for certain configurations, such as the one shown in Box 1, the $+1/2$ defect can propel itself with speed $\sim v_0$ away from the $-1/2$ defect. The balance of elastic and active forces sets a length scale $r_c \sim K/v_0$, beyond which activity always rips apart the defect pair, causing it to inevitably unbind. This simple picture is spoiled by the fact that $+1/2$ defects do not travel in a straight line, rather their direction of motion is affected by rotational noise and changes in the local nematic structure. Unlike the motion of charges driven by an externally applied electric field, the motility of $+1/2$ disclinations is determined by their local geometry. As a result, the $+1/2$ defect has a finite *persistence length* $\ell_p = v_0 \tau_R^{-1}$ beyond which its motion is not ballistic, where τ_R^{-1} controls the rate of rotational noise from active processes. Upon com-

paring this persistence length to the length scale r_c where pair attraction and defect propulsion balance, we get a simple criterion for active defect unbinding [36]. Defect pairs unbind if $\ell_p > r_c$. Conversely, when $\ell_p < r_c$, the $+1/2$ defect changes its direction of motion before overcoming Coulomb attraction, resulting in a local change of the nematic texture that allows the pair to remain bound. It is interesting to note that rotational noise here *stabilizes* the quasi-ordered nematic phase below a finite activity threshold by disrupting the persistent motion of the $+1/2$ defect. This order-from-disorder mechanism highlights the difference between active and driven defects: the latter would inevitably unbind under the action of any external field as nothing disrupts their straight line motion.

Above a critical value of activity, the BKT-like unbinding yields an interacting gas of unbound and swarming defects that provides a useful picture to describe the state of active turbulence. Several models of varying complexity have been proposed for the dynamics of active defects [36, 42, 64, 81, 100–104]. While details differ, the basic physics is the same: the unbound defect gas is a mixture of self-propelled (the $+1/2$ defects) and passive (the $-1/2$ defect) charged particles interacting via Coulomb forces. Recent work has also emphasized the non-reciprocal nature of active defect interactions [104, 105], although its detailed consequences remain to be explored. Coarse-graining over many defects allows a hydrodynamic description of the active defect gas [37, 106], along the lines of previous classic works in the context of superfluid vortices [107] and 2D crystal melting [108]. Importantly, a hydrodynamic treatment of defects offers a theoretical handle on the strongly interacting many-body dynamics of this far-from-equilibrium system. As a crucial ingredient, this description includes a polarization field that captures the average orientation of a collection of active $+1/2$ defects. This field accounts not only for self-propulsion actively driving material flow, but being a vector, the orientation also experiences active torques. When activity is sufficiently strong, and viscous stresses are negligible compared to frictional dissipation with a substrate, one finds that the $+1/2$ defects spontaneously condense into a polar-ordered collectively moving state—a defect flock [37]. The fleeting defects constantly turn over due to creation and annihilation events, but polar order persists for infinitely longer than the individual defect lifetime. Heuristically, such a state arises when the underlying nematic elasticity is too slow to relax the distortion created in the wake of an unbinding defect pair. Similar defect-ordered states have been observed previously in simulations, either with polar ordering [109–112] or defect lattices [113]. Experiments on microtubule-kinesin based active nematic films have reported an extraordinary *nematic* ordered defect state [109]. While continuum simulations recover largely transient nematic defect ordering [111, 114], this observation continues to be a theoretical puzzle. Recent work suggests elastic torques may play a role in antipolar or-

Box 2: Models of active fluids.

Active systems composed of self-propelled units that dissipate energy to create motion and forces can exhibit various collective phases that depend on the symmetry of both the interaction and active motion. Aligning active agents can develop polar (vectorial) and apolar (nematic) orientational order. Scalar active particles can undergo motility-induced phase separation. In this case the order parameter is a scalar, i.e., the density difference between the dense and dilute phases. Active particles may also be chiral and organize in states with macroscopic chirality. While polar and nematic chiral states are also possible, they are not shown here for simplicity. In this box, we primarily focus on fluids and will not discuss active solids and other translationally ordered media.

Active polar fluids

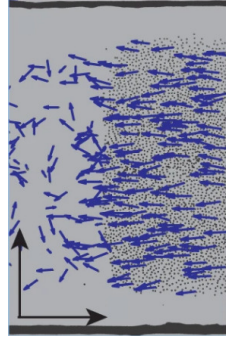
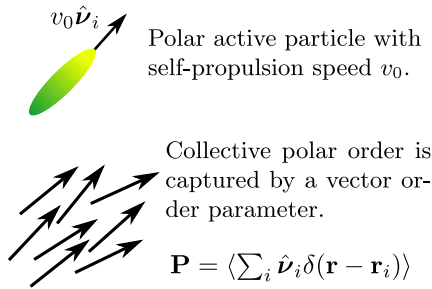


Fig. B1 Polar fluid composed of colloidal rollers (Ref. [5]).

The hydrodynamics of an active polar fluid on a substrate involves the density field (ρ) and the order parameter (\mathbf{P}), and is given by the Toner-Tu equations [52,53].

$$\begin{aligned} \partial_t \rho + v_0 \nabla \cdot (\rho \mathbf{P}) &= 0 \\ \partial_t \mathbf{P} + \lambda \mathbf{P} \cdot \nabla \mathbf{P} &= [a_2 - a_4 |\mathbf{P}|^2] \mathbf{P} + K \nabla^2 \mathbf{P} - \nabla \Pi \end{aligned}$$

Both v_0 and λ are active parameters capturing advection, while a_2, a_4 control the ordering transition with K an elastic constant and a density dependent pressure $\Pi(\rho)$.

Scalar active matter

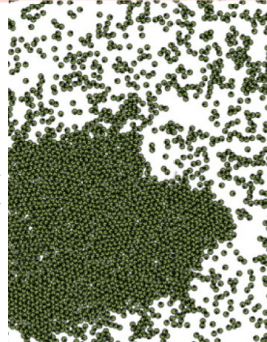
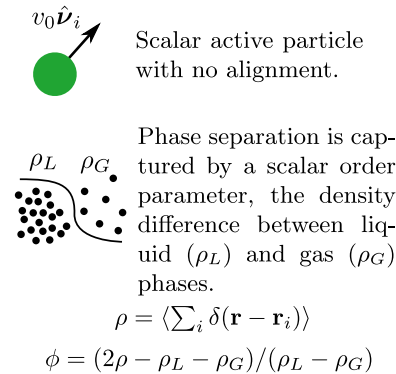


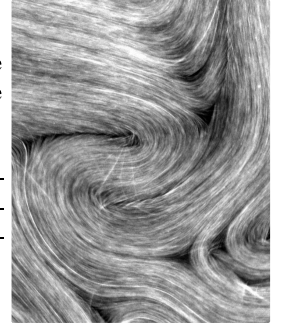
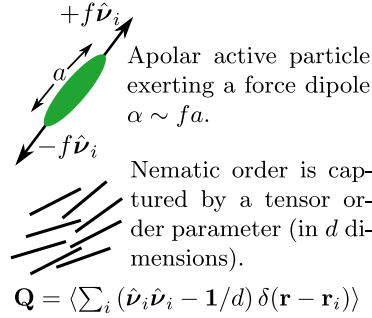
Fig. B3 Simulation of active particles undergoing MIPS. (Ref. [93])

The simplest continuum model of motility-induced phase separation (MIPS) is of Cahn-Hilliard form involving the density (ρ) [92].

$$\begin{aligned} \partial_t \rho &= \nabla \cdot [D(\rho) \nabla \mu] \\ \mu &= \ln[\rho v(\rho)] + \kappa(\rho) \nabla^2 \rho \end{aligned}$$

The effective chemical potential μ includes the density suppression of motility $v(\rho)$ and nonintergrable gradient terms ($\kappa'(\rho) \neq 0$). Density also suppresses the diffusion constant ($D \propto [v(\rho)]^2$).

Active nematic fluids

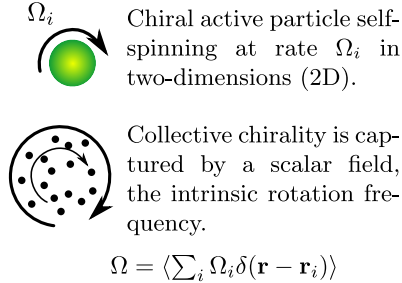


Incompressible active nematics microtubule-minimally couple nematic order (\mathbf{Q}) and flow (\mathbf{u}) driven by an active stress ($\sigma_a = \alpha \mathbf{Q}$) [39].

$$\begin{aligned} \partial_t \mathbf{Q} + \mathbf{u} \cdot \nabla \mathbf{Q} + [\boldsymbol{\omega}, \mathbf{Q}] &= \lambda \mathbf{E} + [a_2 - a_4 S^2] \mathbf{Q} + K \nabla^2 \mathbf{Q} \\ \eta \nabla^2 \mathbf{u} - \Gamma \mathbf{u} + \nabla \cdot \boldsymbol{\sigma}_a - \nabla \Pi &= \mathbf{0} \quad \nabla \cdot \mathbf{u} = 0 \end{aligned}$$

Force balance involves friction (Γ), viscosity (η) and pressure (Π). \mathbf{E} and $\boldsymbol{\omega}$ are symmetric and antisymmetric parts of $\nabla \mathbf{u}$ causing flow alignment (λ). Nematic ordering [$S^2 = \text{tr}(\mathbf{Q}^2)d/(d-1)$] is controlled by a_2, a_4 and the elastic constant K .

Chiral active fluids



The simplest hydrodynamics of an isotropic chiral active fluid in 2D includes density (ρ), flow (\mathbf{u}) and the internal spin density (Ω) [175,182].

Fig. B4 Chiral fluid of colloidal spinning magnets (Ref. [177]).

$$\begin{aligned} \partial_t \rho + \nabla \cdot (\rho \mathbf{u}) &= 0 \\ \partial_t \mathbf{u} &= \eta \nabla^2 \mathbf{u} - \Gamma \mathbf{u} + \eta_R \nabla_{\perp} (2\Omega - \boldsymbol{\omega}) + \eta_o \nabla^2 \mathbf{u}_{\perp} - \nabla \Pi \\ \partial_t \Omega &= \tau_0 - \Gamma_{\Omega} \Omega - 2\eta_R (2\Omega - \boldsymbol{\omega}) + D_{\Omega} \nabla^2 \Omega \end{aligned}$$

Along with regular viscosity (η) and friction (Γ), we also have odd viscosity (η_o) and rotational viscosity (η_R), the latter in the antisymmetric stress. Chirality enters through terms involving $\mathbf{u}_{\perp} = \hat{\mathbf{z}} \times \mathbf{u}$ and the vorticity $\boldsymbol{\omega} = \hat{\mathbf{z}} \cdot (\nabla \times \mathbf{u})$. The active torque (τ_0) injects spin which is damped by spin friction (Γ_{Ω}) and diffusion (D_{Ω}).

dering of defects [115, 116].

Finally, vortex unbinding has been shown to also play a role in disordered polar active fluids [117]. Here, active flows conspire with quenched obstacles to realize a dynamical vortex glass that can be rationalized through an effective Kosterlitz-Thouless-like argument in analogy with dirty superconductors. Generalizing similar ideas to active matter in heterogeneous environments [118] remains an open question.

C. Active defects under confinement

The direct connection between defects and active flows offers new avenues for rectifying and controlling the spontaneous chaotic dynamics of active nematics, paving the way to the application of these system to the development of active microfluidic devices [123]. Active nematic films built by depleting microtubule bundles and kinesin motor complexes onto an oil-water interface [7] have emerged as a versatile platform to manipulate defects by controlling the structure and materials properties of the supporting interface. One simple approach is by tuning the viscosity of the oil layer that hydrodynamically constrains the nematic flow [124]. Other techniques involve the use of more structured environments that can be controlled by external fields and themselves patterned with defects, such as depositing active nematic films onto bulk smectics [97, 121] (Fig. 1h). When in contact with the active nematic layer, focal conic domains in the smectic, for instance, cause the active disclinations to swirl along circular trajectories [97]. In 3D, active drops in a passive nematic fluid can also entrain and activate the dynamics of passive defects, such as ring disclinations in the surrounding nematic [125, 126]. This provides a neat way to rapidly reconfigure and channel flows in the system by rectifying defect motion.

Physical confinement has also been studied, particularly in the disc geometry. Spiral vortices were first stabilized in bacterial suspensions by confinement [127, 128], though their size was limited ($\lesssim 80 - 100 \mu\text{m}$) by the intrinsic instability toward turbulence. High solvent viscoelasticity can “calm” active turbulence and allow larger millimeter-scale bacterial vortices with both coherent and globally oscillating flows [129]. Polar fluids of colloidal rollers, which lack the hydrodynamic interactions that causes bacterial turbulence, self-organize into macroscopically stable vortex pattern when confined to circular tracks [63] and exhibit novel states of pinned vortices in the presence of quenched disorder in the substrate [117] (Fig. 1c). Microtubule-based active nematics also develop steady circulating flow when strongly confined, giving way to a pair of $+1/2$ defects (as topologically required) nucleating at the boundary and orbiting around each other [119, 130]. For large disc sizes, more defects nucleate and unbind in the bulk, degenerating into active turbulence (Fig. 1a). Laterally confined nematics support shear states into which $+1/2$ defects are continually

injected, as they swim around each other in a dancing fashion [131, 132]. While experiments and continuum simulations agree well in many regards, recent work has noted discrepancies in predictions related to defect nucleation and steady flow states in confined nematics [119], suggesting more theoretical work is required.

A third way is to confine active fluids using curved substrates. Curvature frustrates order and often necessitates defects [13], providing an exciting avenue to pattern active fluids. Nematics assembled onto spherical vesicles must accommodate a net topological charge $+2$, as required by the Gauss-Bonnet theorem [133]. In equilibrium, for equal bend and splay elastic constants, the configuration lowest in energy corresponds to four $+1/2$ defects located at the corner of a tetrahedron inscribed by the sphere [134, 135]. In *active* nematic vesicles the four defects are motile and oscillate coherently between two equivalent tetrahedral configurations, driving spontaneous cell-like shape oscillations (Fig. 1b) [64, 100, 136]. On a torus, the spatially varying positive and negative Gaussian curvature causes defects to unbind, attracting disclinations to regions of matching sign curvature [65], thereby filtering them by charge. Polar fluids on a sphere instead form vortices at the poles and a distinctive polar band that concentrates near the equator as a result of active advective fluxes pushing material toward the equator [137, 138].

D. Biological relevance of topological defects

One of the most exciting developments has been the recent characterization of topological defects in living tissues, bacterial colonies and even in multicellular organisms viewed as active materials. Elongated cells can form ordered liquid-crystalline textures interrupted by $\pm 1/2$ disclinations. In confluent epithelial tissues [71] and dense cultures of neural progenitors [72], cells were found to preferentially migrate and accumulate at $+1/2$ disclinations and escape from $-1/2$ disclinations (Fig. 1e). This behavior originates from the large distortion of order around the defect which generates strong local active stresses (Fig. 1f). These large compressive stresses drive cell response, and ultimately lead to cell extrusion and death in epithelia [71]. The structure and role of these active stresses has been confirmed by direct traction force microscopic measurements and via comparison with simulations of active nematic hydrodynamics. Similar phenomena have now been reported in bacterial systems as well. In growing biofilms, $-1/2$ defects instead provide sites for mound formation and buckling [79], while geometrically patterned $+1$ asters have been suggested to support verticalization [80]. Motile bacteria also display related behaviour; for instance, starved myxobacteria use $\pm 1/2$ defects to seed multilayers and cavities to initiate fruiting body formation [77], while slow moving *P. aeruginosa* cells outcompete faster mutants that effectively jam at defects and escape into the third dimension [78].

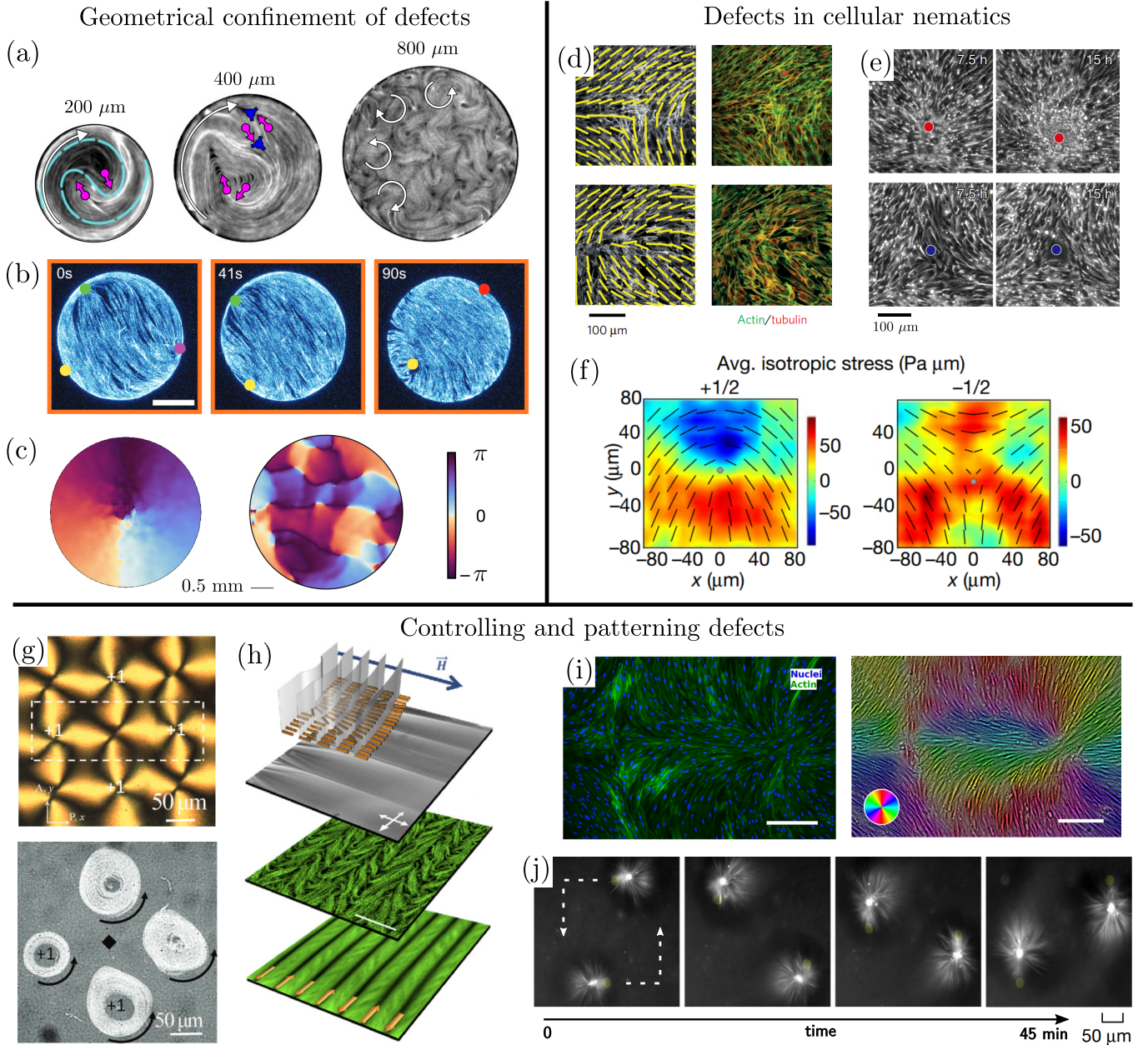


FIG. 1. *Geometrical confinement of defects:* (a) Circulating $+1/2$ defects in a microtubule-kinesin active nematic film confined to a disc ($200 \mu\text{m}$), with more pairs of defects unbinding to create turbulent flows for large disc diameters ($800 \mu\text{m}$) [119]; (b) The same system now condensed onto a spherical vesicle (scale bar, $20 \mu\text{m}$) exhibits periodic oscillations of the four $+1/2$ defects present [64]; (c) Schlieren texture of a colloidal polar fluid in a disc geometry displaying a system-spanning vortex (left) and a pattern of pinned vortex-antivortex pairs (right) induced by randomly located obstacles [117]. *Defects in cellular nematics:* (d) Active $\pm 1/2$ disclinations have been identified in aligned populations of spindle-shaped mouse fibroblasts [69]; (e) Cells accumulate (deplete) at the cores of $+1/2$ ($-1/2$) defects, the former seeding mound formation in dense monolayers of neural progenitor cells [72]; (f) Similar defects in epithelial monolayers of MDCK cells generate large compressive stresses (in blue) only at the head of $+1/2$ disclinations that locally trigger cell extrusion and apoptosis [71]. *Controlling and patterning defects:* (g) Directing vortical polar flows of bacteria dispersed in a nontoxic liquid crystal patterned with a periodic array of alternating ± 1 defects [120]; (h) Passive bulk smectic aligned by an external magnetic field couples hydrodynamically to an adjacent microtubule-kinesin active nematic film, forcing defects to orient and flow along alternating shear bands (scale bar, $100 \mu\text{m}$) [121]; (i) Patterning a tissue of human fibroblast cells (HDF) growing on a liquid crystal elastomer with a pre-designed texture of ± 1 defects (scale bar, $300 \mu\text{m}$) [122]; (j) Time-series of dynamically assembled asters transported along a predetermined trajectory within a bulk microtubule-kinesin suspension, by local light activation [75].

The role of defects in organizing tissue morphogenesis is another exciting frontier. In the context of developing Hydra [73], topological defects in aligned supracellular actomyosin have been shown to correlate with specific morphogenetic processes in regenerating tissue. Remarkably, along with motile $+1/2$ disclinations, stable $+1$ defects emerge at locations coinciding with the eventual mouth and foot of the organism, thereby defining the body axis well before morphological features appear. Recent *in vitro* experiments with confined myoblasts show tornado-like mound morphogenesis at patterned $+1$ asters that provide sites for growth and cellular differentiation [139, 140]. Active defects have also been found to control the dynamic morphologies of growing cell layers [141], 2D bacterial colonies [142, 143], and shape-shifting active shells [144]. We do not yet have general principles to unify these observations, but these results suggest interesting ways in which active defects can constrain or be harnessed to serve diverse evolutionary, developmental, and survival strategies.

On a more subcellular level, the mitotic spindle provides a classic example of a self-organized aster-like defect maintained in constant flux by actin treadmilling and motor activity [145]. Separate from the above, recent *in vivo* experiments on starfish oocytes also demonstrate excitable biochemical spiral waves and defect chaos in the expression of certain membrane bound signalling proteins [146]. While it remains to be seen what the full implications of topological defects to biology are, it is clear that such an approach is highly productive and at the frontier of active matter research.

E. Experimental advances and defect-based control of active matter

Beyond elucidating novel phenomena in nonequilibrium physics lies the challenge of harnessing and controlling them. Active matter experiments have made rapid strides in the past decade and are now poised to engineer reconfigurable and programmable materials. A key strategy is to use topological defects as natural motifs to build dynamic structures with organized flow. Biocompatible liquid crystals perfused with swimming bacteria afford simple static control through prepatterned topological defects (Fig. 1g) that capture bacteria and direct their collective motion based on topological charge [120, 147]. A related strategy has also been employed more recently to pattern defects in aligned epithelial monolayers (Fig. 1i) grown on structured substrates with strong anchoring [122, 148].

Modern advances in engineering optical control of biomolecular activity provide a platform to dynamically control and pattern active materials at will [75, 76, 149]. This has been demonstrated in microtubule-kinesin based gels [75], where local light activation reversibly self-assembles 3D asters dynamically stabilized by the clustering and polarized motion of motor proteins. These de-

fect structures can be moved and arranged in arbitrary patterns in both space and time (Fig. 1j). A similar strategy has also been employed recently in active nematic films to locally pattern active stresses and direct defect motion using spatio-temporal activity gradients [76]. Inhomogeneous activity profiles can act as “electric fields” and drive the sorting of defects by topological charge [37], primarily due to the self-propulsion of $+1/2$ disclinations which accumulate in regions of low activity, unlike non-motile $-1/2$ disclinations. This can be exploited to create defect patterns in active fluids and concomitantly design functional materials with targeted transport capabilities. Defect-based control is poised to create innovative active metamaterials in the future [76, 150], possibly facilitated by data driven techniques [151–153].

II. TOPOLOGICAL BAND STRUCTURES IN ACTIVE MATTER

The topological defects considered so far are robust features of the *order parameter* of active media. We now turn to topologically protected waves whose robustness stems from their *band structures*. In general, a band structure describes the frequencies at which waves (e.g. sound modes) are allowed to propagate as a function of their wavevectors, along with the way the system vibrates at a given frequency. Frequency ranges in which waves are not allowed to propagate are called band gaps. As a simple example, consider a ring filled with air or any other fluid at rest. The clockwise and counterclockwise modes corresponding to density waves in the ring are degenerate, resulting in a point where the bands “touch” in a lattice of such ring resonators. If a fan that circulates the air in a given direction is added to each ring, the degeneracy is broken (a bit like a spin in a magnetic field). As a result a lattice of such circulators will exhibit a band gap rather than a degeneracy [43, 44].

The lattice of circulators exhibits two somewhat surprising properties characteristic of a class of materials called Chern insulators [15, 16]. First, there are so-called edge states, which have frequencies in the bulk gap—the region where bulk modes do not exist—whose existence is guaranteed by topological invariants in the band structure. Second, these edge states propagate only along the boundaries of the material and only in a single direction (because these states arise from breaking of time-reversal invariance).

The construction of the topological invariants controlling this robust edge wave propagation can be intuited via a simple mathematical analogy. When the intrinsic (Gaussian) curvature of a toroid is integrated over the entire surface, the result must always equal zero, independent of the precise shape. This is an example of the Gauss-Bonnet theorem [133], which relates the integrated Gaussian curvature of a closed two-dimensional surface to its genus. This powerful theorem allows us to calculate global topological features of a smooth surface

Box 3: Topological band theory in active fluids: A primer.

Upon linearization, the hydrodynamic models presented in Box 2 generically yield equations of the form

$$\partial_t \mathbf{X} = D\mathbf{X}, \quad (2)$$

in which \mathbf{X} is a vector containing the departure of the hydrodynamic fields from their steady-state values (e.g., $\mathbf{X} = (\rho - \rho_0, \mathbf{u})$ in a chiral active fluid with fixed rotation Ω). To solve Eq. (2), we perform a Fourier transform in

space and time (i.e., $\mathbf{X}(t, \mathbf{r}) \rightarrow \mathbf{X} e^{i(\omega t - \mathbf{q} \cdot \mathbf{r})}$). As an example, consider the spectrum of a chiral active fluid experiencing a Coriolis force $\mathbf{f}_B = \omega_B \mathbf{u}_\perp$ that breaks time-reversal symmetry [175]

$$i\omega \begin{bmatrix} \rho/\rho_0 \\ u_x/c \\ u_y/c \end{bmatrix} = i \begin{bmatrix} 0 & q_x & q_y \\ q_x & 0 & -i(\omega_B - \eta_o q^2) \\ q_y & i(\omega_B - \eta_o q^2) & 0 \end{bmatrix} \begin{bmatrix} \rho/\rho_0 \\ u_x/c \\ u_y/c \end{bmatrix}, \quad (3)$$

where η_o denotes the odd viscosity coefficient discussed in the main text and Box 2. By diagonalizing the dynamical matrix $D(\mathbf{q})$ in Eq. (3), we obtain the dispersion relations $\omega_n(\mathbf{q})$ from its eigenvalues, which are plotted in black in (a). We also obtain the associated eigenvectors $\mathbf{X}_n(\mathbf{q})$ from which we can determine the relevant topological invariant using a standard recipe (see Refs. [17,155] for proofs and generalizations to systems with different spatial dimensions and symmetries). First, calculate the so-called Berry connection $\mathcal{A}_n(\mathbf{q})$ for band n from the eigenvectors $\mathbf{X}_n(\mathbf{q})$ (in a similar fashion to how one calculates the so-called spin connection of a surface [154]):

$$\mathcal{A}_n(\mathbf{q}) = i [\mathbf{X}_n(\mathbf{q})]^\dagger \cdot [\nabla_{\mathbf{q}} \mathbf{X}_n(\mathbf{q})]. \quad (4)$$

Second, determine the Berry curvature (as one would determine the Gaussian curvature from the spin connection [154]):

$$\mathcal{B}_n(\mathbf{q}) = \nabla_{\mathbf{q}} \times \mathcal{A}_n(\mathbf{q}). \quad (5)$$

Third, obtain the relevant topological invariants, called the first Chern numbers \mathcal{C}_n [20] (one per band) using a generalized Gauss-Bonnet formula. These topological indices can be seen as a generalization of the Euler characteristic of a surface [133,154], but with the Gaussian curvature replaced by the Berry curvature:

$$\mathcal{C}_n = \frac{1}{2\pi} \int d\mathbf{q} \mathcal{B}_n(\mathbf{q}). \quad (6)$$

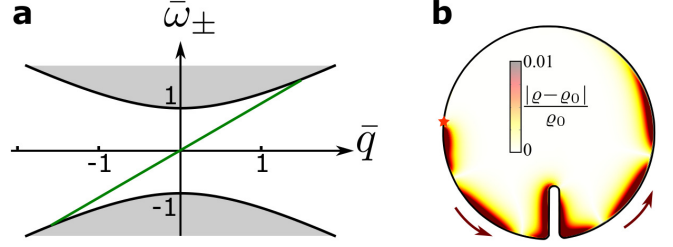
In our example, the first Chern number of the band with positive frequencies is [175]:

$$\mathcal{C}_+ = \text{sign}(\omega_B) + \text{sign}(\eta_o). \quad (7)$$

The existence of non-vanishing first Chern numbers has striking physical consequences at the boundary of the system. In many cases, the algebraic number N of unidirectional modes with frequencies in the bulk band gap at an interface between two systems with Chern numbers \mathcal{C} and \mathcal{C}' is given by:

$$N = \mathcal{C} - \mathcal{C}'. \quad (8)$$

This is called the *bulk-boundary correspondence*. Here, N is the number of modes propagating along the interface from left to right (or clockwise), minus the number of modes going from right to left (or counterclockwise). The band of these chiral edge states can be seen as a green line (with positive slope) spanning the bandgap in Fig. (a). One example of a specific edge state is shown in Fig. (b), which was obtained by driving the edge at a frequency within the bandgap in a fluid dynamic simulation [175]. The Gauss-Bonnet formula directly gives the genus only of compact surfaces without boundary. Similarly, the first Chern numbers in Eq. (6) are only defined under certain conditions: (i) the band n should be well-separated from the others by band gaps and (ii) momentum space should be compact. This is the case for fluids under periodic confinement [175] or thanks to substrate curvature [138,184], but it is not generally guaranteed in fluids. As a consequence, the bulk-boundary correspondence does not always hold [175,178-181,183]. In our example, it is possible to compactify momentum space to get well-defined Chern numbers as long as the quantity η_o (called odd viscosity [175,182]) is non-zero. When η_o vanishes, subtle effects can occur that require thinking outside of (this) Box [158,175,178-181,183]!



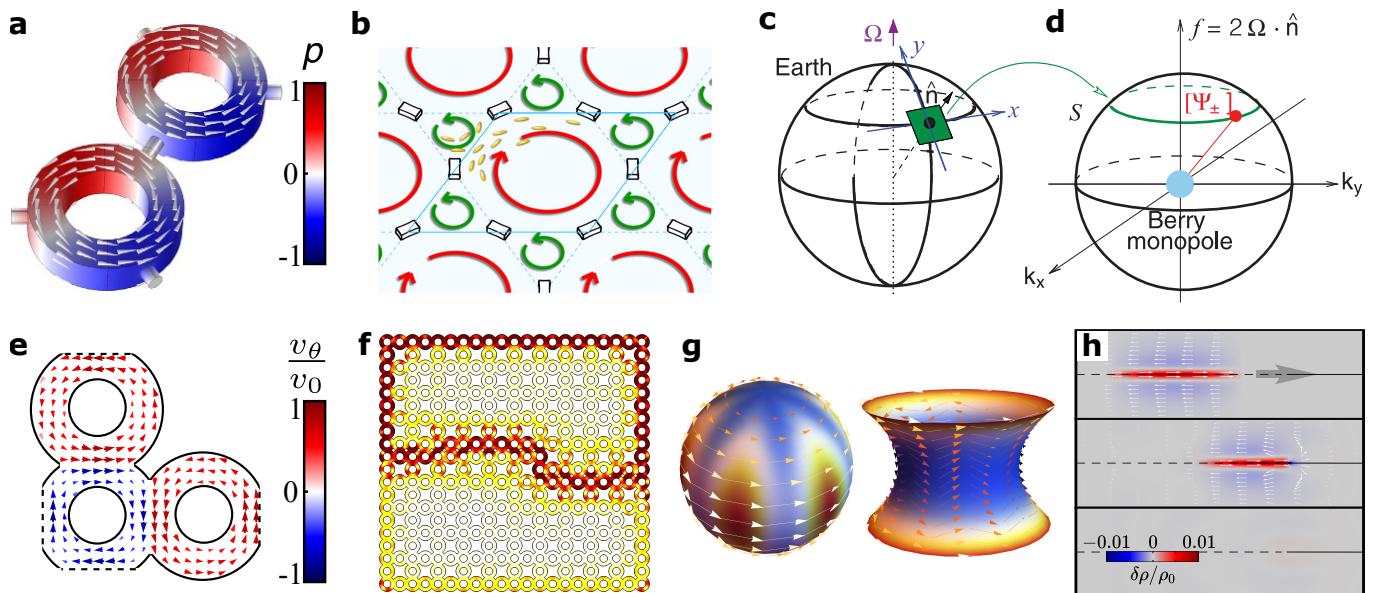


FIG. 2. Topological edge states in fluids far from equilibrium. (a) A topological material based on air driven within circulators in which each unit cell has a net vorticity [43]. (b) A polar active fluid with topological edge states but no net vorticity per unit cell [156]. (c–d) Topological waves on the scale of the Earth in which the equator serves as a boundary along which geophysical waves are topologically protected by a Berry monopole due to the Earth’s overall rotation [157]. (e–f) Phenomenology of topological edge states in a polar active fluid confined inside a Lieb lattice of annuli [45]. Steady state flow (e) and topological density excitations at edges and interfaces of the lattice (f) are shown. (g) Such topologically protected states arise at the equator in a polar active flock confined to the surface of either a sphere (left) or a catenoid (right) [138]. (h) Boundary conditions that do not satisfy bulk-boundary correspondence can be exploited to create perfect absorption: a wavepacket is sent in from the left (top); The wave is absorbed when it encounters a change in boundary conditions (middle), leading to the wavepacket to be entirely absorbed (bottom) [158].

from purely *local* geometric quantities. Analogously, the topological invariants of band structures are obtained by integrating an abstract curvature describing the geometry of eigenvalues and eigenvectors for the linear operator governing wave propagation (Box 3).

Here we review the explanation for how topological band structures result in topologically protected modes at the boundary of a finite sample or at interfaces between systems with topologically distinct band structures. At the edge, the Chern number must go from its value in the bulk of the medium to zero (its value outside of the sample). This change cannot happen smoothly because the Chern number is an integer. What happens instead is that the condition for defining a Chern number, namely that the system is gapped, must cease to be valid at the edge, giving rise to confined wave propagation. The edge states resulting from this mechanism exhibit topological protection: they persist even if the properties of the medium are changed, as long as the bulk gap is not closed. As a consequence, the states exist even if defects, obstacles, or sharp features such as corners are present along the boundary. The waves propagate unabated through and around these obstructions without any backscattering: they cannot go back since the edge mode is unidirectional, and cannot penetrate the gapped bulk.

Topological wave propagation is not unique to active

media. Besides optical and quantum systems [15, 30], it can also occur in mechanical systems such as coupled oscillators [27, 159, 160] as well as simple fluids in circulator arrays [43, 44]. Similar consequences ensue by harnessing active components to induce nontrivial band topology. As examples, a topological solid can be realized using ball-and-spring models with active feedback control [161, 162] or by connecting motorized gyroscopes with springs [163–165]. The combination of the rotation of the gyroscopes and the geometry of the lattice breaks time-reversal symmetry (TRS), and leads to a mechanical Chern insulator with chiral edge states at its boundary. These persist even when some of the gyroscopes are removed or immobilized. In the next subsections, we illustrate the occurrence of topological waves in two classes of active fluids: polar active fluids composed of self-propelled particles and chiral active fluids composed of self-rotating particles.

A. Topological states in confined polar active fluids

Polar fluids naturally break time-reversal symmetry through spontaneous flows, which can be directed by geometric confinement to realize emergent chirality and novel topological edge states. We begin with the example from Ref. [45] of a polar active fluid confined in periodic

microfluidic channels (see Fig. 2e–f). The channel geometry is composed of coupled rings, each reminiscent of an acoustic ring resonator [166] (Fig. 2a). Although the fluid itself is polar and achiral, the annular confinement endows the fluid with a spontaneously broken chiral symmetry, which distinguishes between clockwise (CW) or counterclockwise (CCW) spontaneous flow [63, 127, 167, 168]. For a periodic geometry of rings positioned on a square lattice [169], time-reversal symmetry is restored on average, because there is an equal number of CW and CCW rings. By contrast, removing a single ring from a 2×2 super cell of the square lattice results in a so-called Lieb lattice (with three rings per square unit cell in an L-shaped pattern, Fig. 2e). In this case, time-reversal symmetry is broken on the scale of the unit cell.

This difference between the square and the Lieb lattices has drastic consequences for density waves. Due to the presence of TRS, the square lattice has band crossings at certain symmetric wavevectors. By contrast, TRS is broken in the Lieb lattice and band gaps open between the bands [45]. Each of these gapped bands can be assigned a Chern number C_n (see definition in Box 3) whose value is generically nonzero, and is controlled both by the chirality of the flow and the geometry of the lattice. Note that in other lattices (such as a honeycomb lattice), it is also possible to obtain topological states without a net unit cell vorticity [156]. In the limit in which the speed of flow v is smaller than the speed of sound c , the penetration depth for the localized mode scales as ca/v (where a is the lattice spacing), approaching a if $v \approx c$ [45]. In contrast to driven fluids [43, 44], where achieving this condition requires moderate Mach numbers or resonances, active fluids afford independent control of flow and sound speed, both of which are typically of the same order in experimental realizations [5, 170]. This leads to well-confined edge modes with penetration depth of order lattice spacing. This feature may be technologically advantageous in the design of miniaturized sonic waveguides [45, 171, 172].

Instead of periodic confinement, it is possible to use substrate curvature to produce topological edge states in polar active fluids [138] (Fig. 2g). Gaussian curvature coupled with mean flow breaks Galilean invariance and generically gaps long-wavelength sound modes that acquire a topological character due to the absence of TRS. On the surface of a sphere, a polar active fluid spontaneously circulates around the equator in a chiral fashion [137, 138], experiencing an active analog of the Coriolis force that changes sign across (and vanishes at) the equator. Passive fluids on a rotating sphere, common in geophysical and atmospheric contexts, also exhibit well-known equatorially localized topological sound modes [157] due to the inertial Coriolis force (Fig. 2c–d). In both cases, the equator acts as a gapless interface between two topologically distinct hemispheres. As a result, density waves in a polar active fluid on a spherical surface exhibit unidirectional propagation and topological protection along the equator in addition to the polar

fluid flows [138]. This phenomenon is generic to active flow on any surface with nonzero Gaussian curvature and leads to long-wavelength topological sound modes localized along paths that are both geodesics and flow streamlines (Fig. 2g).

B. Topological waves and odd viscosity in chiral active fluids

In the above examples of polar active fluids, band-structure topology emerges from the spatial environment that the fluid inhabits. Activity primarily serves to break time-reversal symmetry, which allows for non-zero Chern numbers. On the other hand, chiral active fluids exhibit topological states even in the absence of structured confinement (Ref. [175] and Box 3). In this case, activity itself endows the fluid with chirality and mesoscopic lengthscales, leading to topologically protected edge states.

For topological states in chiral fluids, activity needs to simultaneously play two distinct roles: (1) breaking time-reversal symmetry and (2) creating a mesoscopic lengthscale in the fluid response. Consider a bulk chiral active fluid inside a disk. The fluid will spontaneously rotate due to the balance between local torques arising from self-rotating constituents and dissipation, with rigid-body rotation (having angular velocity ω_B) being the preferred steady state over a broad parameter range [175–177] (also see Box 1). This rigid-body rotation not only breaks time-reversal symmetry due to flow, but also opens up a band gap around zero frequency in the fluid bulk. The origin of the band gap is once again rooted in the breaking of a basic symmetry of classical hydrodynamics: Galilean invariance (i.e., constant boosts in velocity leave the system unchanged). Rigid-body rotation breaks Galilean invariance by having a fixed rotation axis, and leads to the presence of a band gap. While polar fluids require confinement to generate rotation [45, 63, 127, 138], chiral active fluids do so intrinsically in the bulk [175–177].

As we explain in Box 3, the Chern number is not always well-defined in fluids [175, 178–181], because the acoustic bands of a fluid are defined on the plane of wavevectors \mathbf{q} which is a non-compact space. This is in contrast with lattice systems, in which the wavevectors are only defined modulo reciprocal lattice vectors (they form a torus called the Brillouin zone, which is compact). In the example described in Box 3, it is possible to replace the plane by a sphere because of the presence of a dissipationless viscosity called odd viscosity (η_o , also see Box 2) that can act as a short distance regularization [175, 177, 180, 182, 183]. A striking feature of chiral active fluids is that the Chern number in Eq. (7) in Box 3 can change without closing the band gap [184]. This jump occurs when η_o changes sign. The band gap does not close because its width is determined solely by the rotation rate ω_B , but the Chern number in Eq. (7) still changes. In this unusual topological phase transition, the

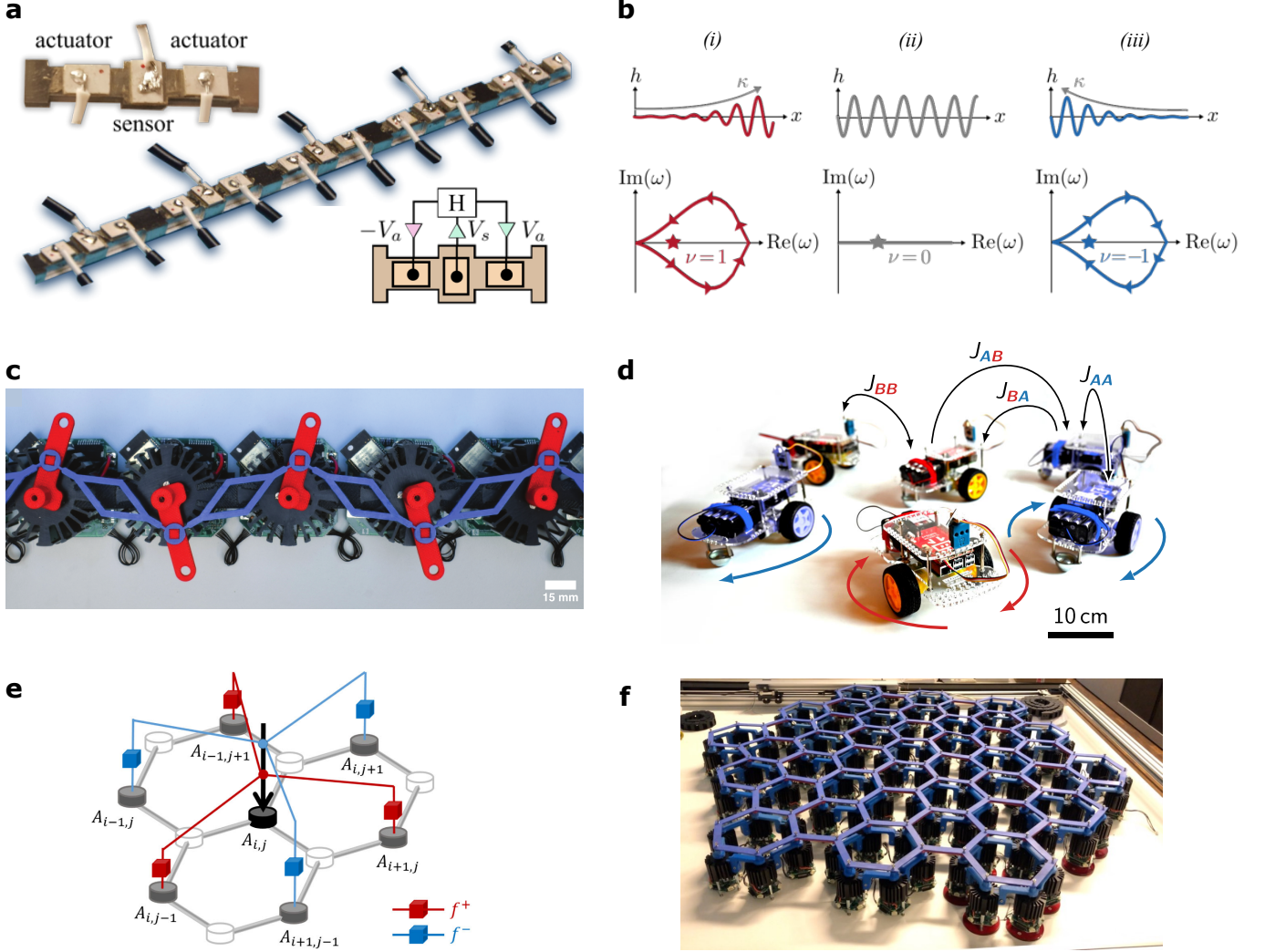


FIG. 3. *Topology and exceptional points in active and robotic metamaterials:* (a) Experimental realization of a self-sensing metabeam with active elasticity. A single unit cell featuring three piezoelectric patches: one that acts as a sensor, and two that act as actuators. Each unit cell has an electronic feedback. (b) Eigenmodes with open periodic boundary conditions with frequency corresponding to the star in the bottom panels. The localization of this eigenmode is determined by the sign of the winding of the energy in the complex plane. Sketches of the spectrum with periodic boundaries for each of the three cases: (i) right, (ii) no, and (iii) left localization. The arrows indicate directions of increasing wave number k . (a–b) are adapted from Ref. [173]. (c) A robotic metamaterial composed of an array of sensors and motors (black, with red rods attached) coupled together by soft elastic beams (blue). The motors enforce non-reciprocal interactions in response to forces exerted by neighbors and detected using the sensors. The edge of this one-dimensional metamaterial realizes modes corresponding to a non-Hermitian skin effect. Adapted from Ref. [174]. (d) A swarm of robots programmed to interact as non-reciprocal spins [33]. Instead of (anti)aligning like an (anti)ferromagnet, they spontaneously rotate either clockwise or counterclockwise, despite having no average natural frequency. The robotic spins are separated in two populations A (blue) and B (red). The intraspecies exchange interaction J_{AA} and J_{BB} are reciprocal, but the interspecies interactions are not, with $J_{AB} \approx -J_{BA}$. If self-propulsion is switched on, non-reciprocal flocking models exhibiting exceptional points are necessary to describe the behavior of the robotic swarm. A time-dependent phase with spontaneously broken chiral symmetry emerges in which self-propelled robots run in circles, either clockwise or counterclockwise, despite the absence of any external torque, adapted from Ref. [33]. (e) A mechanical lattice whose cells are subjected to active feedback forces processed through autonomous controllers can be programmed to generate desired local response in real time including topological edge states, reproduced from Ref. [161]. (f) A robotic metamaterial is built using a honeycomb lattice with robotic joints whose angular deflections are asymmetrically coupled. It exhibits an odd elastic modulus coupling the two shear modes (while maintaining conservation of both linear and angular momentum) and non-Hermitian skin modes (courtesy C. Coulais).

hydrodynamic theory breaks down at short scales as the penetration depth of one of the edge modes goes to zero, and the transition can proceed without band inversion or band gap closure [175]. For the same reason, topological continuum theories also allow for violations of the bulk-boundary correspondence [175, 178–181, 183, 185]. This violation can in turn be exploited to construct waveguides that perfectly absorb a mode in the presence of dissipation (see Fig. 2h) [158].

C. Non-Hermitian band theory in active media

In the previous discussion of topological band theory, we have tacitly assumed that the dynamical matrix D is Hermitian, i.e., $D = D^\dagger$ (or equivalently, perfectly anti-Hermitian, i.e., $D = -D^\dagger$). When this assumption does not hold, the band structure can be literally more complex: the eigenvalues are neither purely real nor purely imaginary. The real and imaginary parts correspond, respectively, to the oscillation frequencies and decay rates of the relevant perturbations (or vice-versa). In addition, we also have assumed that D is a normal operator, i.e., $[D, D^\dagger] = 0$. This is always true if D is Hermitian. When this assumption does not hold, the eigenvectors of D need not be orthogonal to each other, see Box 4. These two changes require generalizations of topological band theory [186–190]. In quantum mechanics, it is natural to assume that the Hamiltonian D of a *closed* system is Hermitian. This restrictive assumption has to be relaxed when studying open quantum systems. Two broad themes have been explored in this context: non-Hermitian skin modes and exceptional points. Before providing an intuitive explanation of these concepts, we stress that their occurrence in classical systems is generic: there is no a priori reason why the linearized operator D should be Hermitian (or even normal), see Box 4.

Consider, as a simple example, the advection-diffusion equation [191]:

$$\partial_t \rho = -v_0 \partial_x \rho + \eta \partial_x^2 \rho, \quad (9)$$

whose Fourier transformed dynamical matrix $D(q_x)$ is just a complex number given by $D(q_x) = iv_0 q_x - \eta q_x^2$ (where q_x is the wavevector). Manifestly, $D(q_x) \neq D^\dagger(q_x)$ since it has both a real and imaginary parts. Here, $D(q_x)$ is normal but not Hermitian. Equation (9) describes the transport of a dye with density ρ in a fluid moving with constant velocity v_0 . When a boundary is inserted in the fluid, the dye accumulates at one end because of the advection v_0 . While hardly a surprising conclusion, this is in fact a very simple manifestation of the non-Hermitian skin effect: a general phenomenon in which the eigenmodes of a non-Hermitian operator are almost all localized to the edge of the system. An iconic example of non-Hermitian quantum mechanics is the so-called Hatano-Nelson model [188], which is essentially a quantum version of Eq. (9). From a classical per-

spective, the asymmetric hopping of electrons (leading to skin modes localized at the edge) in the Hatano-Nelson model can be simply thought as a biased random walk: if the electrons are more likely to hop to the right than to the left, they will accumulate at the right edge. As explained in Box 4, the skin effect is characterized by a non-Hermitian winding number [192–194], a topological invariant distinct from the Chern number discussed in Box 3.

In active media (Fig. 3a–c), various strategies have been devised to generate and control the localization of energy using the non-Hermitian skin effect [173, 186–190, 193–206]. These approaches mostly rely on breaking a family of symmetries collectively known as reciprocity [33, 207–213]. For example, Ref. [201] uses a 1D chain of coupled non-reciprocal robots whose motors effectively violate Newton’s third law (see Fig. 3c). Similar effects have been observed in 1D microfluidic crystals [214] and many other soft and active matter systems in which non-reciprocal interactions naturally emerge as a result of the particles being immersed in a medium or in contact with a substrate or field that provides linear or angular momentum [2, 4, 5, 52, 53, 170, 176, 177, 199, 209–211, 214–230]. In this case, the presence of non-Hermitian skin modes can be rationalized using a simplified heuristic argument. Since the forces (or torques) at the two ends of a non-reciprocal bond are not equal and opposite, there is a net momentum flux across each bond. As a result, momentum or energy accumulates at one of the two ends of an open chain determined by the direction of the force (or torque) imbalance very much like the advected dye described by Eq. (9).

So far, we have explained how violations of linear and/or angular momentum conservation lead to non-reciprocity. Can one achieve similar effects (and the resulting non-Hermitian mechanical response) in a self-standing system not coupled to a substrate or any other momentum source/sink? The answer is yes, for example, when the system is active. To grasp this point, we need to consider a notion of reciprocity that is distinct from Newton’s third law—called Maxwell-Betti reciprocity—which can intuitively be defined as the symmetry between perturbation and response. Let us consider an example in the context of Cauchy elasticity in which the deformation of a solid is described by a strain tensor u_{ij} and the internal forces by a stress tensor σ_{ij} . When a passive or active mechanical system is deformed, the infinitesimal work done is $dW = \sigma_{ij} du_{ij}$. For small perturbations about an undeformed state, the stresses are related to strain deformations through $\sigma_{ij} = C_{ijkl} u_{kl}$ in which C_{ijkl} is the tensor of elastic moduli. If the stress-strain relation can be derived from a free energy $V = \frac{1}{2} C_{ijkl} u_{ij} u_{kl}$, then the stiffness tensor C_{ijkl} is symmetric, i.e., $C_{ijkl} = C_{klij}$. This symmetry is called Maxwell-Betti reciprocity [32].

When the microscopic forces are not conservative, Maxwell-Betti reciprocity is in general violated because $C_{ijkl} \neq C_{klij}$, and additional active elastic moduli are present, which we refer to as odd elasticity [231]. As a

Box 4: Non-Hermitian band theory: \mathcal{PT} symmetry, exceptional points and skin modes.

In active systems, the dynamical matrix D defined in Box 3 is not always Hermitian (or even normal). Hence, its eigenvalues $s = \omega - i\sigma$ are not necessarily real: there can be a growth/decay rate σ in addition to the oscillation frequency ω . In general, the eigenvalues of D are real if and only if there is an antiunitary operator O , with $O^2 = \text{Id}$, that commutes with the dynamical matrix D and such that the eigenvectors ψ_i of D satisfy $O\psi_i = \psi_i$. The operator O is a symmetry of the dynamical matrix, called generalized \mathcal{PT} -symmetry for historical reasons [189]. A situation can arise when O commutes with D while simultaneously $O\psi_i \neq \psi_i$ for at least one of the eigenvectors of D . In this case, the (generalized) \mathcal{PT} -symmetry is said to be spontaneously broken (it is *unbroken* when $O\psi_i = \psi_i$ for all i). The notion of \mathcal{PT} symmetry can be thought of as a generalization of the statement that the eigenvalues of a real matrix must come in complex conjugate pairs. When all the eigenvalues are real, the \mathcal{PT} symmetry is unbroken, otherwise it is broken. To see this structure in a familiar context, consider the damped harmonic oscillator (a) described by the non-normal matrix

$$\begin{bmatrix} \dot{p} \\ \dot{x} \end{bmatrix} = \begin{bmatrix} -\Gamma/M & -k \\ 1/M & 0 \end{bmatrix} \begin{bmatrix} p \\ x \end{bmatrix}, \quad (10)$$

where M is the mass, Γ the damping coefficient and k the spring constant. Transitions between \mathcal{PT} -unbroken and \mathcal{PT} -broken states are generically accompanied by exceptional points, where the two eigenvectors coalesce (red lines in b). For the harmonic oscillator, the exceptional point occurs at critical damping separating the overdamped and underdamped regimes. An active example is given by solids whose bonds are described by the non-conservative force law $\mathbf{F}(\mathbf{r}) = -(k\hat{\mathbf{r}} + k^a\hat{\phi})\delta r$ where $\hat{\mathbf{r}}$ ($\hat{\phi}$) is a unit vector pointing along (transverse to) the bond vector, δr is the change in length of the bond, and k and k^a are spring constants (c) [231]. When the bond is taken on a closed cycle, the work done $W = \oint \mathbf{F} \cdot d\mathbf{r}$ is equal to k^a times the area enclosed by the path. The dynamical matrix that governs the motion of a single particle in the trap shown in (d) exhibits an exceptional point at a critical value of $k_a/k = 1/\sqrt{3}$. Similar phenomena occur in *overdamped* solids made of non-conservative bonds whose linear evolution can be expressed through a non-normal dynamical matrix via

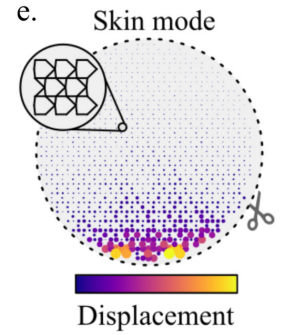
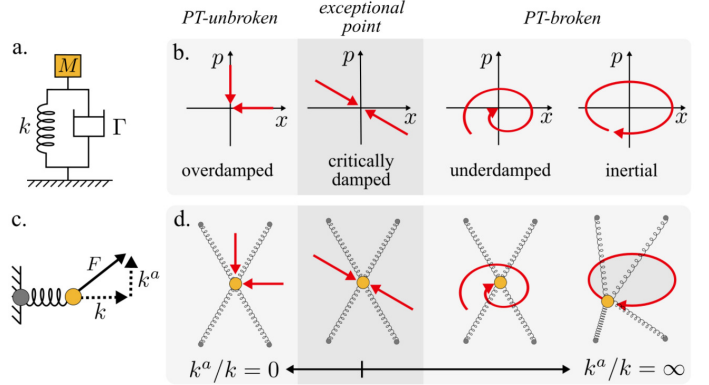
$$\Gamma \begin{bmatrix} \dot{u}_{\parallel} \\ \dot{u}_{\perp} \end{bmatrix} = q^2 \begin{bmatrix} B + \mu & K^o \\ -K^o & \mu \end{bmatrix} \begin{bmatrix} u_{\parallel} \\ u_{\perp} \end{bmatrix}. \quad (11)$$

Here, $u_{\parallel}(\mathbf{q})$ and $u_{\perp}(\mathbf{q})$ indicate the Fourier modes of the longitudinal and transverse displacement field. The coefficients B and μ are the bulk and shear moduli, while K^o and A are two additional active moduli [231] that exist in 2D isotropic media. Exceptional points in \mathcal{PT} symmetric systems generically mark the crossover between oscillating and strictly relaxing behaviors. In some cases, e.g., the active spring and simple harmonic oscillator, this transition can be easily visualized as a crossover between linear and circular motion [198].

The ability of non-Hermitian systems to host non-orthogonal eigenvectors gives rise to striking vibrational features such as the non-Hermitian skin effect [174,195,198,205], see Fig. e. Unlike Hermitian topological edge modes, in which a subextensive number of modes are localized to the boundary, non-Hermitian systems exhibit skin modes that are extensive in number. Given a number λ in the complex plane, it is useful to introduce a winding number number, $\nu(\lambda)$ [173,192]:

$$\nu(\lambda) \equiv \frac{1}{2\pi i} \int_0^{2\pi/a} \frac{d}{dq} \ln \det[D(q) - \lambda] dq, \quad (12)$$

where a is the lattice spacing. When ν is nonzero, a semi-infinite system will host a mode at the complex frequency λ localized at, say, the left or right boundary depending on the sign of ν . In Fig. 3b, for instance, the frequency of a skin mode in an active beam (star) is encircled by the periodic boundary spectrum (solid line). The non-Hermitian invariant ν distinguishes inequivalent paths in the complex eigenvalue plane whereas the Chern number \mathcal{C} measures the winding of the eigenstates (Box 3).



consequence, the dynamical matrix $D_{it}(\mathbf{q}) = C_{ijkl}q_jq_k$ describing the propagation of elastic waves (see Box 4) is not Hermitian, allowing for the appearance of wave propagation in overdamped solids [231] as well as the presence of the skin effect [198]. Figure 3 shows two realizations of metamaterials with odd elasticity: an active metabeam with asymmetric coupling between shearing and bending [173] and a honeycomb lattice with robotic joints whose angular deflections are asymmetrically coupled [232]. In both systems, the skin effect has been observed. Its existence has been also inferred from either lattice models [199–201, 233] or from continuum equations based only on symmetries and conservation laws [173, 198]. Besides synthetic metamaterial or colloidal systems [173, 232, 234], odd elastic responses have recently been reported in living chiral crystals self-assembled from swimming starfish embryos [235].

Up to this point, we have mostly focused on the eigenvalues of non-Hermitian dynamical matrices. Yet, the corresponding eigenvectors play as crucial a role. When the dynamical matrix D is not normal, it is not always enough to know the eigenvalues to assess the linear stability of the system. This is because the eigenvectors can fail to be orthogonal to each other with respect to the physically relevant scalar product, e.g., a quadratic potential energy density. The extreme limit of this failure occurs when two (or more) eigenvectors become collinear: this is called an exceptional point [236]. As a consequence, there can be a transient amplification of perturbations that can drastically affect the stability of the system [191]. A simple example of exceptional points occurs in the damped harmonic oscillator: the overdamped and underdamped regimes are separated by an exceptional point at critical damping (see Box 4). The same thing occurs in active metamaterials: odd elastic waves start propagating when the eigenvalues of D go from being real (decay) to occurring in complex conjugate pairs (oscillations). This transition can be viewed as a spontaneous breaking of a symmetry called \mathcal{PT} symmetry, see Box 4. Tangible physical effects occur near exceptional points as a consequence of the non-normality of D . For instance, there can be a transient amplification of noise and perturbations that can drastically affect the stability of the system [33, 191, 219, 237–239]. When the dynamical matrix D is viewed as a differential operator in real space, its normality also depends on the boundary conditions. The skin effect occurs precisely when the eigenmodes of a system are orthogonal Fourier modes for a system with periodic boundaries, but become non-orthogonal localized modes in a semi-infinite or finite system. Exceptional points can also mediate unusual phase transitions in active many-body systems with non-reciprocal interactions [33, 212, 213].

III. OUTLOOK

Notions from topology and geometry offer a new perspective on active matter and provide unconventional tools for classifying the complex behavior of these far-from-equilibrium systems. Although abstract, topological techniques are becoming increasingly commonplace in the study of active systems. The success of topology, just as in equilibrium materials, is rooted in the identification of robust collective degrees of freedom and excitations, which in active matter often acquire dramatic properties.

Exploring the relevance of topological properties of active systems to biology is perhaps one of the most ambitious avenues in the field. While defects in tissues have been noted as mechanically active centers of morphogenesis [71–73, 77], our understanding of the interplay between active forcing and tissue response in manipulating cell organization is still limited. Integrating biologically relevant mechanisms such as growth, cell differentiation, and mechanotransduction with the physics of active fluids would be crucial to this end. On a different scale, although biofilament-motor assemblies routinely display defects when reconstituted *in-vitro* [7, 40, 55, 240, 241], the relation of these phenomena to *in-vivo* cortical organization [145, 146, 242] remains mysterious and continues to be an open question. During development at the organ and organismal level, both collective motion and pattern formation are ubiquitous [243, 244], which offers an intriguing possibility for the realization of exotic topologically protected states. Recent studies have also suggested a role for topological states in nonequilibrium stochastic [245], excitable [246–249], and evolutionary dynamics [250] networks. One challenge faced by future theoretical work is the robustness of topological states to biologically relevant perturbations. In this regard, more systematic experimental investigations are needed.

Active metamaterials and synthetic active matter offer a broad platform to engineer and apply novel topological states [8, 120]. Controlling and patterning defects using activity gradients has already emerged as an exciting direction of research [37, 75, 76]. While the main focus so far has been on two-dimensional systems, topological states in three dimensions offer new possibilities, including more complex defect textures [87] and topological degeneracies in band structure such as Weyl nodes [251, 252]. Designing synthetic gauge fields [45, 117, 253] and exceptional points in active fluids and solids [33, 198, 231] would be a powerful strategy to exploit these states for sensing and transport. Active flow is already being exploited, for example, to enhance *in-vitro* fertilization [254, 255], and creating topologically protected transport could be a route toward new technologies based on active matter.

From a theoretical perspective, important questions remain. Beyond topological band theory, the role of nonequilibrium noise and nonlinear interactions within

active materials remains largely unexplored [33, 212, 213]. As discussed extensively, topological defects in active systems acquire much of their novelty from their dynamics [39]. Although much work has been done, a detailed understanding of defect-driven phase transitions and exotic defect-ordered states remain elusive. Toward this end, comparing and contrasting active defects with the novel collective dynamics of vortices in open quantum systems and driven dissipative condensates [256–258] promises to be a fruitful endeavor.

ACKNOWLEDGMENTS

The work of MJB was supported in part by the National Science Foundation under Grant No. NSF PHY-1748958 and NSF DMREF program, via Grant No. DMREF-1435794. MCM was primarily supported by the National Science Foundation under Grant No. DMR-2041459, with additional support from DMR-1720256 (iSuperSeed). SS is supported by the Harvard Society

of Fellows. VV was supported by the Complex Dynamics and Systems Program of the Army Research Office under grant W911NF-19-1-0268, by the Simons Foundation and by the University of Chicago Materials Research Science and Engineering Center, which is funded by the National Science Foundation under award number DMR-2011854. SS and AS gratefully acknowledge discussions during the 2019 summer workshop on “Active and Driven Matter: Connecting Quantum and Classical Systems” at the Aspen Center for Physics, which is supported by National Science Foundation grant PHY-1607611. The participation of AS at the Aspen Center for Physics was supported by the Simons Foundation. AS acknowledges the support of the Engineering and Physical Sciences Research Council (EPSRC) through New Investigator Award No. EP/T000961/1. We also acknowledge illuminating discussions throughout the virtual 2020 KITP program on “Symmetry, Thermodynamics and Topology in Active Matter”, which was supported in part by the National Science Foundation under Grant No. NSF PHY-1748958. We thank M. Fruchart, C. Scheibner, G. Baardink, and J. Binysh for inspiring conversations and suggestions.

-
- [1] Ramaswamy, S. The mechanics and statistics of active matter. *Annu. Rev. Condens. Matter Phys.* **1**, 323–345 (2010).
 - [2] Marchetti, M. C. *et al.* Hydrodynamics of soft active matter. *Reviews of Modern Physics* **85**, 1143 (2013).
 - [3] Ramaswamy, S. Active matter. *Journal of Statistical Mechanics: Theory and Experiment* **2017**, 054002 (2017).
 - [4] Palacci, J., Sacanna, S., Steinberg, A. P., Pine, D. J. & Chaikin, P. M. Living crystals of light-activated colloidal surfers. *Science* **339**, 936–940 (2013).
 - [5] Bricard, A., Caussin, J.-B., Desreumaux, N., Dauchot, O. & Bartolo, D. Emergence of macroscopic directed motion in populations of motile colloids. *Nature* **503**, 95 (2013).
 - [6] Schaller, V., Weber, C., Semmrich, C., Frey, E. & Bausch, A. R. Polar patterns of driven filaments. *Nature* **467**, 73–77 (2010).
 - [7] Sanchez, T., Chen, D. T., DeCamp, S. J., Heymann, M. & Dogic, Z. Spontaneous motion in hierarchically assembled active matter. *Nature* **491**, 431–434 (2012).
 - [8] Needleman, D. & Dogic, Z. Active matter at the interface between materials science and cell biology. *Nature Reviews Materials* **2**, 17048 (2017).
 - [9] Cavagna, A. & Giardina, I. Bird flocks as condensed matter. *Annu. Rev. Condens. Matter Phys.* **5**, 183–207 (2014).
 - [10] Trepát, X. & Sahai, E. Mesoscale physical principles of collective cell organization. *Nature Physics* **14**, 671–682 (2018).
 - [11] Mermin, N. D. The topological theory of defects in ordered media. *Reviews of Modern Physics* **51**, 591 (1979).
 - [12] Alexander, G. P., Chen, B. G.-g., Matsumoto, E. A. & Kamien, R. D. Colloquium: Disclination loops, point defects, and all that in nematic liquid crystals. *Reviews of Modern Physics* **84**, 497 (2012).
 - [13] Nelson, D. R. *Defects and geometry in condensed matter physics* (Cambridge University Press, 2002).
 - [14] Kohmoto, M. Topological invariant and the quantization of the hall conductance. *Annals of Physics* **160**, 343–354 (1985).
 - [15] Hasan, M. Z. & Kane, C. L. Colloquium: topological insulators. *Reviews of Modern Physics* **82**, 3045 (2010).
 - [16] Qi, X.-L. & Zhang, S.-C. Topological insulators and superconductors. *Reviews of Modern Physics* **83**, 1057 (2011).
 - [17] Fruchart, M. & Carpentier, D. An introduction to topological insulators. *Comptes Rendus Physique* **14**, 779 – 815 (2013).
 - [18] Halperin, B. I. Quantized hall conductance, current-carrying edge states, and the existence of extended states in a two-dimensional disordered potential. *Physical Review B* **25**, 2185 (1982).
 - [19] Moore, J. E. The birth of topological insulators. *Nature* **464**, 194 (2010).
 - [20] Nakahara, M. *Geometry, topology and physics* (Taylor & Francis, 2003).
 - [21] Ran, Y., Zhang, Y. & Vishwanath, A. One-dimensional topologically protected modes in topological insulators with lattice dislocations. *Nature Physics* **5**, 298–303 (2009).
 - [22] Teo, J. C. & Kane, C. L. Topological defects and gapless modes in insulators and superconductors. *Physical Review B* **82**, 115120 (2010).
 - [23] Juričić, V., Mesáros, A., Slager, R.-J. & Zaanen, J. Universal probes of two-dimensional topological insulators: dislocation and π flux. *Physical review letters* **108**, 106403 (2012).

- [24] Paulose, J., Chen, B. G.-g. & Vitelli, V. Topological modes bound to dislocations in mechanical metamaterials. *Nature Physics* **11**, 153–156 (2015).
- [25] Chaikin, P. M. & Lubensky, T. C. *Principles of condensed matter physics* (Cambridge university press, 2000).
- [26] Zhang, X., Xiao, M., Cheng, Y., Lu, M.-H. & Christensen, J. Topological sound. *Communications Physics* **1**, 1–13 (2018).
- [27] Huber, S. D. Topological mechanics. *Nature Physics* **12**, 621 (2016).
- [28] Khanikaev, A. B. & Shvets, G. Two-dimensional topological photonics. *Nature Photonics* **11**, 763 (2017).
- [29] Mao, X. & Lubensky, T. C. Maxwell lattices and topological mechanics. *Annual Review of Condensed Matter Physics* **9**, 413–433 (2018).
- [30] Ozawa, T. *et al.* Topological photonics. *Reviews of Modern Physics* **91**, 015006 (2019).
- [31] Ma, G., Xiao, M. & Chan, C. T. Topological phases in acoustic and mechanical systems. *Nature Reviews Physics* **1**, 281–294 (2019).
- [32] Nassar, H. *et al.* Nonreciprocity in acoustic and elastic materials. *Nature Reviews Materials* 1–19 (2020).
- [33] Fruchart, M., Hanai, R., Littlewood, P. B. & Vitelli, V. Non-reciprocal phase transitions. *Nature* **592**, 363–369 (2021).
- [34] Seifert, U. From stochastic thermodynamics to thermodynamic inference. *Annual Review of Condensed Matter Physics* **10**, 171–192 (2019).
- [35] Gnesotto, F., Mura, F., Gladrow, J. & Broedersz, C. P. Broken detailed balance and non-equilibrium dynamics in living systems: a review. *Reports on Progress in Physics* **81**, 066601 (2018).
- [36] Shankar, S., Ramaswamy, S., Marchetti, M. C. & Bowick, M. J. Defect unbinding in active nematics. *Phys. Rev. Lett.* **121**, 108002 (2018).
- [37] Shankar, S. & Marchetti, M. C. Hydrodynamics of active defects: from order to chaos to defect ordering. *Physical Review X* **9**, 041047 (2019).
- [38] Ramaswamy, S., Simha, R. A. & Toner, J. Active nematics on a substrate: Giant number fluctuations and long-time tails. *EPL (Europhysics Letters)* **62**, 196 (2003).
- [39] Doostmohammadi, A., Ignés-Mullol, J., Yeomans, J. M. & Sagués, F. Active nematics. *Nature communications* **9**, 3246 (2018).
- [40] Kumar, N., Zhang, R., de Pablo, J. J. & Gardel, M. L. Tunable structure and dynamics of active liquid crystals. *Science Advances* **4**, eaat7779 (2018).
- [41] Narayan, V., Ramaswamy, S. & Menon, N. Long-lived giant number fluctuations in a swarming granular nematic. *Science* **317**, 105–108 (2007). Also see Supporting Information, page 4.
- [42] Giomi, L., Bowick, M. J., Ma, X. & Marchetti, M. C. Defect annihilation and proliferation in active nematics. *Physical review letters* **110**, 228101 (2013).
- [43] Khanikaev, A. B., Fleury, R., Mousavi, S. H. & Alu, A. Topologically robust sound propagation in an angular-momentum-biased graphene-like resonator lattice. *Nature communications* **6**, 1–7 (2015).
- [44] Yang, Z. *et al.* Topological acoustics. *Physical review letters* **114**, 114301 (2015).
- [45] Souslov, A., van Zuiden, B. C., Bartolo, D. & Vitelli, V. Topological sound in active-liquid metamaterials. *Nature Physics* **13**, 1091 (2017).
- [46] Berezinskii, V. Destruction of long-range order in one-dimensional and two-dimensional systems having a continuous symmetry group i. classical systems. *Soviet Journal of Experimental and Theoretical Physics* **32**, 493 (1971). [ZhETF 59, 907 (1971)].
- [47] Berezinskii, V. Destruction of long-range order in one-dimensional and two-dimensional systems possessing a continuous symmetry group ii. quantum systems. *Soviet Journal of Experimental and Theoretical Physics* **34**, 610 (1972). [ZhETF 61, 1144 (1972)].
- [48] Kosterlitz, J. M. & Thouless, D. J. Ordering, metastability and phase transitions in two-dimensional systems. *Journal of Physics C: Solid State Physics* **6**, 1181 (1973).
- [49] Kosterlitz, J. The critical properties of the two-dimensional xy model. *Journal of Physics C: Solid State Physics* **7**, 1046 (1974).
- [50] Kosterlitz, J. M. Kosterlitz–thouless physics: a review of key issues. *Reports on Progress in Physics* **79**, 026001 (2016).
- [51] Vicsek, T., Czirók, A., Ben-Jacob, E., Cohen, I. & Shochet, O. Novel type of phase transition in a system of self-driven particles. *Physical Review Letters* **75**, 1226–1229 (1995).
- [52] Toner, J. & Tu, Y. Long-range order in a two-dimensional dynamical xy model: how birds fly together. *Physical Review Letters* **75**, 4326 (1995).
- [53] Toner, J. & Tu, Y. Flocks, herds, and schools: A quantitative theory of flocking. *Physical review E* **58**, 4828 (1998).
- [54] Toner, J., Tu, Y. & Ramaswamy, S. Hydrodynamics and phases of flocks. *Annals of Physics* **318**, 170–244 (2005).
- [55] Nédélec, F., Surrey, T., Maggs, A. C. & Leibler, S. Self-organization of microtubules and motors. *Nature* **389**, 305 (1997).
- [56] Surrey, T., Nédélec, F., Leibler, S. & Karsenti, E. Physical properties determining self-organization of motors and microtubules. *Science* **292**, 1167–1171 (2001).
- [57] Simha, R. A. & Ramaswamy, S. Hydrodynamic fluctuations and instabilities in ordered suspensions of self-propelled particles. *Physical review letters* **89**, 058101 (2002).
- [58] Voituriez, R., Joanny, J.-F. & Prost, J. Spontaneous flow transition in active polar gels. *EPL (Europhysics Letters)* **70**, 404 (2005).
- [59] Duclos, G. *et al.* Spontaneous shear flow in confined cellular nematics. *Nature physics* **14**, 728–732 (2018).
- [60] Sumino, Y. *et al.* Large-scale vortex lattice emerging from collectively moving microtubules. *Nature* **483**, 448–452 (2012).
- [61] Schaller, V. & Bausch, A. R. Topological defects and density fluctuations in collectively moving systems. *Proceedings of the National Academy of Sciences* **110**, 4488–4493 (2013).
- [62] Köster, D. V. *et al.* Actomyosin dynamics drive local membrane component organization in an in vitro active composite layer. *Proceedings of the National Academy of Sciences* **113**, E1645–E1654 (2016).
- [63] Bricard, A. *et al.* Emergent vortices in populations of colloidal rollers. *Nature communications* **6**, 1–8 (2015).
- [64] Keber, F. C. *et al.* Topology and dynamics of active nematic vesicles. *Science* **345**, 1135–1139 (2014).

- [65] Ellis, P. W. *et al.* Curvature-induced defect unbinding and dynamics in active nematic toroids. *Nature Physics* **14**, 85 (2018).
- [66] Gruler, H., Dewald, U. & Eberhardt, M. Nematic liquid crystals formed by living amoeboid cells. *The European Physical Journal B-Condensed Matter and Complex Systems* **11**, 187–192 (1999).
- [67] Kemkemer, R., Kling, D., Kaufmann, D. & Gruler, H. Elastic properties of nematoid arrangements formed by amoeboid cells. *The European Physical Journal E* **1**, 215–225 (2000).
- [68] Zhou, S., Sokolov, A., Lavrentovich, O. D. & Aranson, I. S. Living liquid crystals. *Proceedings of the National Academy of Sciences* **111**, 1265–1270 (2014).
- [69] Duclos, G., Erenkämper, C., Joanny, J.-F. & Silberzan, P. Topological defects in confined populations of spindle-shaped cells. *Nature Physics* **13**, 58 (2017).
- [70] Blanch-Mercader, C. *et al.* Turbulent dynamics of epithelial cell cultures. *Physical review letters* **120**, 208101 (2018).
- [71] Saw, T. B. *et al.* Topological defects in epithelia govern cell death and extrusion. *Nature* **544**, 212 (2017).
- [72] Kawaguchi, K., Kageyama, R. & Sano, M. Topological defects control collective dynamics in neural progenitor cell cultures. *Nature* **545**, 327 (2017).
- [73] Maroudas-Sacks, Y. *et al.* Topological defects in the nematic order of actin fibers as organization centers of hydra morphogenesis. *bioRxiv preprint bioRxiv 2020.03.02.972539* (2020).
- [74] Giomi, L. Geometry and topology of turbulence in active nematics. *Physical Review X* **5**, 031003 (2015).
- [75] Ross, T. D. *et al.* Controlling organization and forces in active matter through optically defined boundaries. *Nature* **572**, 224–229 (2019).
- [76] Zhang, R. *et al.* Spatiotemporal control of liquid crystal structure and dynamics through activity patterning. *Nature Materials* **20**, 875–882 (2021).
- [77] Copenhagen, K., Alert, R., Wingreen, N. S. & Shaevitz, J. W. Topological defects promote layer formation in myxococcus xanthus colonies. *Nature Physics* **17**, 211–215 (2021).
- [78] Meacock, O. J., Doostmohammadi, A., Foster, K. R., Yeomans, J. M. & Durham, W. M. Bacteria solve the problem of crowding by moving slowly. *Nature Physics* **17**, 205–210 (2021).
- [79] Yaman, Y. I., Demir, E., Vetter, R. & Kocabas, A. Emergence of active nematics in chaining bacterial biofilms. *Nature communications* **10**, 1–9 (2019).
- [80] Başaran, M., Yaman, Y. I., Vetter, R. & Kocabas, A. Formation of self-assembled asters in growing bacterial colonies. *arXiv preprint arXiv:2008.05545* (2020).
- [81] Pismen, L. Dynamics of defects in an active nematic layer. *Physical Review E* **88**, 050502 (2013).
- [82] Maitra, A. & Lenz, M. Spontaneous rotation can stabilise ordered chiral active fluids. *Nature communications* **10**, 1–6 (2019).
- [83] Hoffmann, L. A., Schakenraad, K., Merks, R. M. & Giomi, L. Chiral stresses in nematic cell monolayers. *Soft Matter* (2020).
- [84] Kruse, K., Joanny, J.-F., Jülicher, F., Prost, J. & Sekimoto, K. Asters, vortices, and rotating spirals in active gels of polar filaments. *Physical review letters* **92**, 078101 (2004).
- [85] Shendruk, T. N., Thijssen, K., Yeomans, J. M. & Doostmohammadi, A. Twist-induced crossover from two-dimensional to three-dimensional turbulence in active nematics. *Physical Review E* **98**, 010601 (2018).
- [86] Čopar, S., Aplinc, J., Kos, Ž., Žumer, S. & Ravnik, M. Topology of three-dimensional active nematic turbulence confined to droplets. *Physical Review X* **9**, 031051 (2019).
- [87] Duclos, G. *et al.* Topological structure and dynamics of three-dimensional active nematics. *Science* **367**, 1120–1124 (2020).
- [88] Binysh, J., Kos, Ž., Čopar, S., Ravnik, M. & Alexander, G. P. Three-dimensional active defect loops. *Physical Review Letters* **124**, 088001 (2020).
- [89] Whitfield, C. A. *et al.* Hydrodynamic instabilities in active cholesteric liquid crystals. *The European Physical Journal E* **40**, 50 (2017).
- [90] Metselaar, L., Doostmohammadi, A. & Yeomans, J. M. Topological states in chiral active matter: Dynamic blue phases and active half-skyrmions. *The Journal of chemical physics* **150**, 064909 (2019).
- [91] Carezza, L. N., Gonnella, G., Marenduzzo, D. & Negro, G. Rotation and propulsion in 3d active chiral droplets. *Proceedings of the National Academy of Sciences* **116**, 22065–22070 (2019).
- [92] Cates, M. E. & Tailleur, J. Motility-induced phase separation. *Annu. Rev. Condens. Matter Phys.* **6**, 219–244 (2015).
- [93] Marchetti, M. C., Fily, Y., Henkes, S., Patch, A. & Yllanes, D. Minimal model of active colloids highlights the role of mechanical interactions in controlling the emergent behavior of active matter. *Current Opinion in Colloid & Interface Science* **21**, 34–43 (2016).
- [94] Thampi, S. P., Golestanian, R. & Yeomans, J. M. Velocity correlations in an active nematic. *Physical review letters* **111**, 118101 (2013).
- [95] Wensink, H. H. *et al.* Meso-scale turbulence in living fluids. *Proceedings of the National Academy of Sciences* **109**, 14308–14313 (2012).
- [96] Hemingway, E. J., Mishra, P., Marchetti, M. C. & Fielding, S. M. Correlation lengths in hydrodynamic models of active nematics. *Soft Matter* **12**, 7943–7952 (2016).
- [97] Guillamat, P., Ignés-Mullol, J. & Sagués, F. Taming active turbulence with patterned soft interfaces. *Nature communications* **8**, 564 (2017).
- [98] Lemma, L. M., DeCamp, S. J., You, Z., Giomi, L. & Dogic, Z. Statistical properties of autonomous flows in 2d active nematics. *Soft matter* **15**, 3264–3272 (2019).
- [99] Alert, R., Casademunt, J. & Joanny, J.-F. Active turbulence. *arXiv preprint arXiv:2104.02122* (2021).
- [100] Khoromskaia, D. & Alexander, G. P. Vortex formation and dynamics of defects in active nematic shells. *New Journal of Physics* **19**, 103043 (2017).
- [101] Cortese, D., Eggers, J. & Liverpool, T. B. Pair creation, motion, and annihilation of topological defects in two-dimensional nematic liquid crystals. *Physical Review E* **97**, 022704 (2018).
- [102] Tang, X. & Selinger, J. V. Theory of defect motion in 2d passive and active nematic liquid crystals. *Soft Matter* **15**, 587–601 (2019).
- [103] Zhang, Y.-H., Deserno, M., Tu, Z.-C. *et al.* Dynamics of active nematic defects on the surface of a sphere. *Physical Review E* **102**, 012607 (2020).

- [104] Vafa, F., Bowick, M. J., Marchetti, M. C. & Shraiman, B. I. Multi-defect dynamics in active nematics. *arXiv preprint arXiv:2007.02947* (2020).
- [105] Maitra, A., Lenz, M. & Voituriez, R. Chiral active hexatics: Giant number fluctuations, waves, and destruction of order. *Physical Review Letters* **125**, 238005 (2020).
- [106] Angheluta, L., Chen, Z., Marchetti, M. C. & Bowick, M. J. The role of fluid flow in the dynamics of active nematic defects. *New Journal of Physics* **23**, 033009 (2021).
- [107] Ambegaokar, V., Halperin, B., Nelson, D. R. & Siggia, E. D. Dynamics of superfluid films. *Physical Review B* **21**, 1806 (1980).
- [108] Zippelius, A., Halperin, B. & Nelson, D. R. Dynamics of two-dimensional melting. *Physical Review B* **22**, 2514 (1980).
- [109] DeCamp, S. J., Redner, G. S., Baskaran, A., Hagan, M. F. & Dogic, Z. Orientational order of motile defects in active nematics. *Nature materials* **14**, 1110–1115 (2015).
- [110] Putzig, E., Redner, G. S., Baskaran, A. & Baskaran, A. Instabilities, defects, and defect ordering in an overdamped active nematic. *Soft matter* **12**, 3854–3859 (2016).
- [111] Srivastava, P., Mishra, P. & Marchetti, M. C. Negative stiffness and modulated states in active nematics. *Soft Matter* **12**, 8214–8225 (2016).
- [112] Patelli, A., Djafer-Cherif, I., Aranson, I. S., Bertin, E. & Chaté, H. Understanding dense active nematics from microscopic models. *Physical Review Letters* **123**, 258001 (2019).
- [113] Doostmohammadi, A., Adamer, M. F., Thampi, S. P. & Yeomans, J. M. Stabilization of active matter by flow-vortex lattices and defect ordering. *Nature communications* **7**, 1–9 (2016).
- [114] Oza, A. U. & Dunkel, J. Antipolar ordering of topological defects in active liquid crystals. *New Journal of Physics* **18**, 093006 (2016).
- [115] Pearce, D. *et al.* Scale-free defect ordering in passive and active nematics. *arXiv preprint arXiv:2004.13704* (2020).
- [116] Thijssen, K., Nejad, M. R. & Yeomans, J. M. Role of friction in multidefect ordering. *Physical Review Letters* **125**, 218004 (2020).
- [117] Chardac, A., Shankar, S., Marchetti, M. C. & Bartolo, D. Emergence of dynamic vortex glasses in disordered polar active fluids. *Proceedings of the National Academy of Sciences* **118**, e2018218118 (2021).
- [118] Bechinger, C. *et al.* Active particles in complex and crowded environments. *Reviews of Modern Physics* **88**, 045006 (2016).
- [119] Opatthalage, A. *et al.* Self-organized dynamics and the transition to turbulence of confined active nematics. *Proceedings of the National Academy of Sciences* **116**, 4788–4797 (2019).
- [120] Peng, C., Turiv, T., Guo, Y., Wei, Q.-H. & Lavrentovich, O. D. Command of active matter by topological defects and patterns. *Science* **354**, 882–885 (2016).
- [121] Guillamat, P., Ignés-Mullol, J. & Sagués, F. Control of active liquid crystals with a magnetic field. *Proceedings of the National Academy of Sciences* **113**, 5498–5502 (2016).
- [122] Turiv, T. *et al.* Topology control of human fibroblast cells monolayer by liquid crystal elastomer. *Science Advances* **6**, eaaz6485 (2020).
- [123] Green, R., Toner, J. & Vitelli, V. Geometry of thresholdless active flow in nematic microfluidics. *Phys. Rev. Fluids* **2**, 104201 (2017).
- [124] Guillamat, P., Ignés-Mullol, J., Shankar, S., Marchetti, M. C. & Sagués, F. Probing the shear viscosity of an active nematic film. *Physical Review E* **94**, 060602 (2016).
- [125] Guillamat, P. *et al.* Active nematic emulsions. *Science advances* **4**, eaao1470 (2018).
- [126] Rajabi, M., Baza, H., Turiv, T. & Lavrentovich, O. D. Directional self-locomotion of active droplets enabled by nematic environment. *Nature Physics* **17**, 260–266 (2021).
- [127] Wioland, H., Woodhouse, F. G., Dunkel, J., Kessler, J. O. & Goldstein, R. E. Confinement stabilizes a bacterial suspension into a spiral vortex. *Physical review letters* **110**, 268102 (2013).
- [128] Lushi, E., Wioland, H. & Goldstein, R. E. Fluid flows created by swimming bacteria drive self-organization in confined suspensions. *Proceedings of the National Academy of Sciences* **111**, 9733–9738 (2014).
- [129] Liu, S., Shankar, S., Marchetti, M. C. & Wu, Y. Viscoelastic control of spatiotemporal order in bacterial active matter. *Nature* **590**, 80–84 (2021).
- [130] Norton, M. M. *et al.* Insensitivity of active nematic liquid crystal dynamics to topological constraints. *Physical Review E* **97**, 012702 (2018).
- [131] Shendruk, T. N., Doostmohammadi, A., Thijssen, K. & Yeomans, J. M. Dancing disclinations in confined active nematics. *Soft Matter* **13**, 3853–3862 (2017).
- [132] Hardoüin, J. *et al.* Reconfigurable flows and defect landscape of confined active nematics. *Communications Physics* **2**, 1–9 (2019).
- [133] Carmo, M. P. d. *Riemannian geometry* (Birkhäuser, 1992).
- [134] Nelson, D. R. Toward a tetravalent chemistry of colloids. *Nano Letters* **2**, 1125–1129 (2002).
- [135] Shin, H., Bowick, M. J. & Xing, X. Topological defects in spherical nematics. *Physical review letters* **101**, 037802 (2008).
- [136] Zhang, R., Zhou, Y., Rahimi, M. & De Pablo, J. J. Dynamic structure of active nematic shells. *Nature communications* **7**, 1–9 (2016).
- [137] Sknepnek, R. & Henkes, S. Active swarms on a sphere. *Physical Review E* **91**, 022306 (2015).
- [138] Shankar, S., Bowick, M. J. & Marchetti, M. C. Topological sound and flocking on curved surfaces. *Physical Review X* **7**, 031039 (2017).
- [139] Guillamat, P., Blanch-Mercader, C., Kruse, K. & Roux, A. Integer topological defects organize stresses driving tissue morphogenesis. *bioRxiv* (2020).
- [140] Blanch-Mercader, C., Guillamat, P., Roux, A. & Kruse, K. Quantifying material properties of cell monolayers by analyzing integer topological defects. *Physical Review Letters* **126**, 028101 (2021).
- [141] Comelles, J. *et al.* Epithelial colonies in vitro elongate through collective effects. *Elife* **10**, e57730 (2021).
- [142] Doostmohammadi, A., Thampi, S. P. & Yeomans, J. M. Defect-mediated morphologies in growing cell colonies. *Physical review letters* **117**, 048102 (2016).
- [143] Dell’Arciprete, D. *et al.* A growing bacterial colony in two dimensions as an active nematic. *Nature communi-*

- cations* **9**, 1–9 (2018).
- [144] Metselaar, L., Yeomans, J. M. & Doostmohammadi, A. Topology and morphology of self-deforming active shells. *Physical Review Letters* **123**, 208001 (2019).
- [145] Brugués, J. & Needleman, D. Physical basis of spindle self-organization. *Proceedings of the National Academy of Sciences* **111**, 18496–18500 (2014).
- [146] Tan, T. H. *et al.* Topological turbulence in the membrane of a living cell. *Nature Physics* 1–6 (2020).
- [147] Genkin, M. M., Sokolov, A., Lavrentovich, O. D. & Aranson, I. S. Topological defects in a living nematic ensnare swimming bacteria. *Physical Review X* **7**, 011029 (2017).
- [148] Endresen, K. D., Kim, M., Pittman, M., Chen, Y. & Serra, F. Topological defects of integer charge in cell monolayers. *Soft Matter* (2021).
- [149] Schuppler, M., Keber, F. C., Kröger, M. & Bausch, A. R. Boundaries steer the contraction of active gels. *Nature communications* **7**, 1–10 (2016).
- [150] Norton, M. M., Grover, P., Hagan, M. F. & Fraden, S. Optimal control of active nematics. *Physical Review Letters* **125**, 178005 (2020).
- [151] Li, H. *et al.* Data-driven quantitative modeling of bacterial active nematics. *Proceedings of the National Academy of Sciences* **116**, 777–785 (2019).
- [152] Colen, J. *et al.* Machine learning active-nematic hydrodynamics. *Proceedings of the National Academy of Sciences* **118** (2021).
- [153] Zhou, Z. *et al.* Machine learning forecasting of active nematics. *Soft matter* **17**, 738–747 (2021).
- [154] Kamien, R. D. The geometry of soft materials: a primer. *Reviews of Modern Physics* **74**, 953 (2002).
- [155] Asbóth, J. K., Oroszlány, L. & Pályi, A. *A Short Course on Topological Insulators* (Springer International Publishing, 2016).
- [156] Sone, K. & Ashida, Y. Anomalous topological active matter. *Physical Review Letters* **123**, 205502 (2019).
- [157] Delplace, P., Marston, J. & Venaille, A. Topological origin of equatorial waves. *Science* **358**, 1075–1077 (2017).
- [158] Baardink, G., Cassella, G., Neville, L., Milewski, P. A. & Souslov, A. Complete absorption of topologically protected waves (2020). arXiv:2010.07342.
- [159] Prodan, E. & Prodan, C. Topological phonon modes and their role in dynamic instability of microtubules. *Physical review letters* **103**, 248101 (2009).
- [160] Bertoldi, K., Vitelli, V., Christensen, J. & van Hecke, M. Flexible mechanical metamaterials. *Nature Reviews Materials* **2**, 1–11 (2017).
- [161] Sirota, L., Ilan, R., Shokef, Y. & Lahini, Y. Non-newtonian topological mechanical metamaterials using feedback control. *Phys. Rev. Lett.* **125**, 256802 (2020).
- [162] Sirota, L., Sabsovich, D., Lahini, Y., Ilan, R. & Shokef, Y. Real-time steering of curved sound beams in a feedback-based topological acoustic metamaterial. *Mechanical Systems and Signal Processing* **153**, 107479 (2021).
- [163] Nash, L. M. *et al.* Topological mechanics of gyroscopic metamaterials. *Proceedings of the National Academy of Sciences* **112**, 14495–14500 (2015).
- [164] Wang, P., Lu, L. & Bertoldi, K. Topological phononic crystals with one-way elastic edge waves. *Physical Review Letters* **115**, 104302 (2015).
- [165] Mitchell, N. P., Nash, L. M., Hexner, D., Turner, A. M. & Irvine, W. T. M. Amorphous topological insulators constructed from random point sets. *Nature Physics* **14**, 380–385 (2018).
- [166] Fleury, R., Sounas, D. L., Sieck, C. F., Haberman, M. R. & Alù, A. Sound isolation and giant linear nonreciprocity in a compact acoustic circulator. *Science* **343**, 516–519 (2014).
- [167] Stenhammar, J., Wittkowski, R., Marenduzzo, D. & Cates, M. E. Light-induced self-assembly of active rectification devices. *Science advances* **2**, e1501850 (2016).
- [168] Thampi, S. P., Doostmohammadi, A., Shendruk, T. N., Golestanian, R. & Yeomans, J. M. Active micromachines: Microfluidics powered by mesoscale turbulence. *Science advances* **2**, e1501854 (2016).
- [169] Wioland, H., Woodhouse, F. G., Dunkel, J. & Goldstein, R. E. Ferromagnetic and antiferromagnetic order in bacterial vortex lattices. *Nature physics* **12**, 341–345 (2016).
- [170] Geyer, D., Morin, A. & Bartolo, D. Sounds and hydrodynamics of polar active fluids. *Nature materials* **17**, 789–793 (2018).
- [171] Cha, J., Kim, K. W. & Daraio, C. Experimental realization of on-chip topological nanoelectromechanical metamaterials. *Nature* **564**, 229–233 (2018).
- [172] Cummer, S. A., Christensen, J. & Alù, A. Controlling sound with acoustic metamaterials. *Nature Reviews Materials* **1**, 16001 (2016).
- [173] Chen, Y., Li, X., Scheibner, C., Vitelli, V. & Huang, G. Self-sensing metamaterials with odd micropolarity. *arXiv preprint arxiv.2009.07329* (2020).
- [174] Brandenbourger, M., Locsin, X., Lerner, E. & Coullais, C. Non-reciprocal robotic metamaterials. *Nature communications* **10**, 1–8 (2019).
- [175] Souslov, A., Dasbiswas, K., Fruchart, M., Vaikunathan, S. & Vitelli, V. Topological waves in fluids with odd viscosity. *Physical review letters* **122**, 128001 (2019).
- [176] van Zuiden, B. C., Paulose, J., Irvine, W. T., Bartolo, D. & Vitelli, V. Spatiotemporal order and emergent edge currents in active spinner materials. *Proceedings of the national academy of sciences* **113**, 12919–12924 (2016).
- [177] Soni, V. *et al.* The odd free surface flows of a colloidal chiral fluid. *Nature Physics* **15**, 1188–1194 (2019).
- [178] Silveirinha, M. G. Proof of the bulk-edge correspondence through a link between topological photonics and fluctuation-electrodynamics. *Physical Review X* **9**, 011037 (2019).
- [179] Volovik, G. An analog of the quantum hall effect in a superfluid he-3 film. *Soviet Physics-JETP* **67**, 1804–1811 (1988).
- [180] Tauber, C., Delplace, P. & Venaille, A. Anomalous bulk-edge correspondence in continuous media. *Physical Review Research* **2**, 013147 (2020).
- [181] Tauber, C., Delplace, P. & Venaille, A. A bulk-interface correspondence for equatorial waves. *Journal of Fluid Mechanics* **868** (2019).
- [182] Banerjee, D., Souslov, A., Abanov, A. G. & Vitelli, V. Odd viscosity in chiral active fluids. *Nature communications* **8**, 1–12 (2017).
- [183] Bal, G. Continuous bulk and interface description of topological insulators. *Journal of Mathematical Physics* **60**, 081506 (2019).
- [184] A change in the Chern number without a band gap closing is also possible in polar active fluids on curved sub-

- strates, when the density and orientational sound speeds become equal, causing Galilean invariance to effectively be restored [138]. However, this mechanism is unrelated to any short scale regularization.
- [185] Bal, G. Topological invariants for interface modes. *arXiv preprint arXiv:1906.08345* (2019).
- [186] Budich, J. C., Carlström, J., Kunst, F. K. & Bergholtz, E. J. Symmetry-protected nodal phases in non-hermitian systems. *Phys. Rev. B* **99**, 041406 (2019).
- [187] Ashida, Y., Gong, Z. & Ueda, M. Non-hermitian physics. *Advances in Physics* **69**, 249–435 (2020).
- [188] Hatano, N. & Nelson, D. R. Localization transitions in non-hermitian quantum mechanics. *Phys. Rev. Lett.* **77**, 570–573 (1996).
- [189] Bender, C. M. & Boettcher, S. Real spectra in non-hermitian hamiltonians having pt symmetry. *Phys. Rev. Lett.* **80**, 5243–5246 (1998).
- [190] Bergholtz, E. J., Budich, J. C. & Kunst, F. K. Exceptional topology of non-hermitian systems. *Reviews of Modern Physics* **93**, 015005 (2021).
- [191] Trefethen, L. N. & Embree, M. *Spectra and Pseudospectra* (Princeton University Press, 2005).
- [192] Gong, Z. *et al.* Topological phases of non-hermitian systems. *Physical Review X* **8**, 031079 (2018).
- [193] Zhang, K., Yang, Z. & Fang, C. Correspondence between winding numbers and skin modes in non-hermitian systems. *Phys. Rev. Lett.* **125**, 126402 (2020).
- [194] Okuma, N., Kawabata, K., Shiozaki, K. & Sato, M. Topological origin of non-hermitian skin effects. *Phys. Rev. Lett.* **124**, 086801 (2020).
- [195] Yao, S. & Wang, Z. Edge states and topological invariants of non-hermitian systems. *Physical review letters* **121**, 086803 (2018).
- [196] Weidemann, S. *et al.* Topological funneling of light. *Science* **368**, 311–314 (2020).
- [197] Lee, C. H. & Thomale, R. Anatomy of skin modes and topology in non-hermitian systems. *Phys. Rev. B* **99**, 201103 (2019).
- [198] Scheibner, C., Irvine, W. T. & Vitelli, V. Non-hermitian band topology and skin modes in active elastic media. *Physical Review Letters* **125**, 118001 (2020).
- [199] Rosa, M. I. & Ruzzene, M. Dynamics and topology of non-hermitian elastic lattices with non-local feedback control interactions. *New Journal of Physics* **22**, 053004 (2020).
- [200] Zhou, D. & Zhang, J. Non-hermitian topological metamaterials with odd elasticity. *Phys. Rev. Research* **2**, 023173 (2020).
- [201] Ghatak, A., Brandenbourger, M., van Wezel, J. & Coulais, C. Observation of non-hermitian topology and its bulk–edge correspondence in an active mechanical metamaterial. *Proceedings of the National Academy of Sciences* **117**, 29561–29568 (2020).
- [202] Borgnia, D. S., Kruchkov, A. J. & Slager, R.-J. Non-hermitian boundary modes and topology. *Physical Review Letters* **124**, 056802 (2020).
- [203] Schomerus, H. Nonreciprocal response theory of non-hermitian mechanical metamaterials: Response phase transition from the skin effect of zero modes. *Physical Review Research* **2**, 013058 (2020).
- [204] Thust, T. Flow-induced non-hermitian topology in ordinary elastic matter. *arXiv preprint arXiv:2102.04184* (2021).
- [205] Yamauchi, L., Hayata, T., Uwamichi, M., Ozawa, T. & Kawaguchi, K. Chirality-driven edge flow and non-hermitian topology in active nematic cells (2020). arXiv:2008.10852.
- [206] Palacios, L. S. *et al.* Guided accumulation of active particles by topological design of a second-order skin effect. *arXiv preprint arXiv:2012.14496* (2020).
- [207] Das, J., Rao, M. & Ramaswamy, S. Driven heisenberg magnets: Nonequilibrium criticality, spatiotemporal chaos and control. *Europhysics Letters (EPL)* **60**, 418–424 (2002).
- [208] Lahiri, R. & Ramaswamy, S. Are steadily moving crystals unstable? *Physical Review Letters* **79**, 1150–1153 (1997).
- [209] Uchida, N. & Golestanian, R. Synchronization and collective dynamics in a carpet of microfluidic rotors. *Physical Review Letters* **104**, 178103 (2010).
- [210] Saha, S., Ramaswamy, S. & Golestanian, R. Pairing, waltzing and scattering of chemotactic active colloids. *New Journal of Physics* **21**, 063006 (2019).
- [211] Gupta, R. K., Kant, R., Soni, H., Sood, A. & Ramaswamy, S. Active nonreciprocal attraction between motile particles in an elastic medium. *arXiv preprint arXiv:2007.04860* (2020).
- [212] You, Z., Baskaran, A. & Marchetti, M. C. Nonreciprocity as a generic route to traveling states. *Proceedings of the National Academy of Sciences* **117**, 19767–19772 (2020).
- [213] Saha, S., Agudo-Canalejo, J. & Golestanian, R. Scalar active mixtures: The nonreciprocal cahn-hilliard model. *Physical Review X* **10**, 041009 (2020).
- [214] Beatus, T., Thust, T. & Bar-Ziv, R. Phonons in a one-dimensional microfluidic crystal. *Nature Physics* **2**, 743–748 (2006).
- [215] Kumar, N., Soni, H., Ramaswamy, S. & Sood, A. Flocking at a distance in active granular matter. *Nature communications* **5**, 1–9 (2014).
- [216] Baek, Y., Solon, A. P., Xu, X., Nikola, N. & Kafri, Y. Generic long-range interactions between passive bodies in an active fluid. *Phys. Rev. Lett.* **120**, 058002 (2018).
- [217] Ivlev, A. V. *et al.* Statistical mechanics where newton’s third law is broken. *Phys. Rev. X* **5**, 011035 (2015).
- [218] Lavergne, F. A., Wendehenne, H., Bäuerle, T. & Bechinger, C. Group formation and cohesion of active particles with visual perception-dependent motility. *Science* **364**, 70–74 (2019).
- [219] Chajwa, R., Menon, N., Ramaswamy, S. & Govindarajan, R. Waves, algebraic growth, and clumping in sedimenting disk arrays. *Physical Review X* **10**, 041016 (2020).
- [220] Kryuchkov, N. P., Ivlev, A. V. & Yurchenko, S. O. Dissipative phase transitions in systems with nonreciprocal effective interactions. *Soft Matter* **14**, 9720–9729 (2018).
- [221] Yifat, Y. *et al.* Reactive optical matter: light-induced motility in electro-dynamically asymmetric nanoscale scatterers. *Light: Science & Applications* **7**, 105 (2018).
- [222] Peterson, C. W., Parker, J., Rice, S. A. & Scherer, N. F. Controlling the dynamics and optical binding of nanoparticle homodimers with transverse phase gradients. *Nano Letters* **19**, 897–903 (2019).
- [223] Morin, A., Caussin, J.-B., Eloy, C. & Bartolo, D. Collective motion with anticipation: Flocking, spinning, and swarming. *Phys. Rev. E* **91**, 012134 (2015).

- [224] Dadhichi, L. P., Kethapelli, J., Chajwa, R., Ramaswamy, S. & Maitra, A. Nonmutual torques and the unimportance of motility for long-range order in two-dimensional flocks. *Phys. Rev. E* **101**, 052601 (2020).
- [225] Barberis, L. & Peruani, F. Large-scale patterns in a minimal cognitive flocking model: Incidental leaders, nematic patterns, and aggregates. *Phys. Rev. Lett.* **117**, 248001 (2016).
- [226] Loos, S. A. M., Hermann, S. M. & Klapp, S. H. L. Non-reciprocal hidden degrees of freedom: A unifying perspective on memory, feedback, and activity (2019). 1910.08372.
- [227] Bain, N. & Bartolo, D. Dynamic response and hydrodynamics of polarized crowds. *Science* **363**, 46–49 (2019).
- [228] Bertin, E., Droz, M. & Grégoire, G. Boltzmann and hydrodynamic description for self-propelled particles. *Phys. Rev. E* **74**, 022101 (2006).
- [229] Farrell, F. D. C., Marchetti, M. C., Marenduzzo, D. & Tailleur, J. Pattern formation in self-propelled particles with density-dependent motility. *Phys. Rev. Lett.* **108**, 248101 (2012).
- [230] Mishra, S., Baskaran, A. & Marchetti, M. C. Fluctuations and pattern formation in self-propelled particles. *Phys. Rev. E* **81**, 061916 (2010).
- [231] Scheibner, C. *et al.* Odd elasticity. *Nature Physics* 1–6 (2020).
- [232] Brandenbourger, M., Scheibner, C., Veenstra, J., Vitelli, V. & Coulais, C. Active impact and locomotion in robotic metamaterials. *in preparation* (2021).
- [233] Gao, P., Willatzen, M. & Christensen, J. Anomalous topological edge states in non-hermitian piezophononic media. *Physical Review Letters* **125**, 206402 (2020).
- [234] Bililign, E. S. *et al.* Chiral crystals self-knead into whorls. *arXiv preprint arXiv:2102.03263* (2021).
- [235] Tan, T. H. *et al.* Development drives dynamics of living chiral crystals. *arXiv preprint arXiv:2105.07507* (2021).
- [236] Heiss, W. The physics of exceptional points. *Journal of Physics A: Mathematical and Theoretical* **45**, 444016 (2012).
- [237] Trefethen, L. N., Trefethen, A. E., Reddy, S. C. & Driscoll, T. A. Hydrodynamic stability without eigenvalues. *Science* **261**, 578–584 (1993).
- [238] Hanai, R. & Littlewood, P. B. Critical fluctuations at a many-body exceptional point. *Physical Review Research* **2**, 033018 (2020).
- [239] Strack, P. & Vitelli, V. Soft quantum vibrations of a PT-symmetric nonlinear ion chain. *Physical Review A* **88**, 053408 (2013).
- [240] Edozie, B. *et al.* Self-organization of spindle-like microtubule structures. *Soft Matter* **15**, 4797–4807 (2019).
- [241] Weirich, K. L., Dasbiswas, K., Witten, T. A., Vaikuntanathan, S. & Gardel, M. L. Self-organizing motors divide active liquid droplets. *Proceedings of the National Academy of Sciences* **116**, 11125–11130 (2019).
- [242] Gowrishankar, K. *et al.* Active remodeling of cortical actin regulates spatiotemporal organization of cell surface molecules. *Cell* **149**, 1353–1367 (2012).
- [243] Lecuit, T. & Mahadevan, L. Morphogenesis one century after on growth and form (2017).
- [244] Howard, J., Grill, S. W. & Bois, J. S. Turing’s next steps: the mechanochemical basis of morphogenesis. *Nature Reviews Molecular Cell Biology* **12**, 392–398 (2011).
- [245] Murugan, A. & Vaikuntanathan, S. Topologically protected modes in non-equilibrium stochastic systems. *Nature communications* **8**, 1–6 (2017).
- [246] Kotwal, T. *et al.* Active topoelectrical circuits. *arXiv preprint arXiv:1903.10130* (2019).
- [247] Hofmann, T., Helbig, T., Lee, C. H., Greiter, M. & Thomale, R. Chiral voltage propagation and calibration in a topoelectrical chern circuit. *Physical review letters* **122**, 247702 (2019).
- [248] Helbig, T. *et al.* Generalized bulk–boundary correspondence in non-hermitian topoelectrical circuits. *Nature Physics* 1–4 (2020).
- [249] Ronellenfitsch, H. & Dunkel, J. Spectral design of active mechanical and electrical metamaterials. In *2020 Fourteenth International Congress on Artificial Materials for Novel Wave Phenomena (Metamaterials)*, 270–272 (IEEE, 2020).
- [250] Knebel, J., Geiger, P. M. & Frey, E. Topological phase transition in coupled rock-paper-scissors cycles. *Physical Review Letters* **125**, 258301 (2020).
- [251] Armitage, N., Mele, E. & Vishwanath, A. Weyl and dirac semimetals in three-dimensional solids. *Reviews of Modern Physics* **90**, 015001 (2018).
- [252] Fruchart, M. *et al.* Soft self-assembly of weyl materials for light and sound. *Proceedings of the National Academy of Sciences* **115**, E3655–E3664 (2018).
- [253] Abbaszadeh, H., Souslov, A., Paulose, J., Schomerus, H. & Vitelli, V. Sonic landau levels and synthetic gauge fields in mechanical metamaterials. *Physical Review Letters* **119**, 195502 (2017).
- [254] Denissenko, P., Kantsler, V., Smith, D. J. & Kirkman-Brown, J. Human spermatozoa migration in microchannels reveals boundary-following navigation. *Proceedings of the National Academy of Sciences* **109**, 8007–8010 (2012).
- [255] Kantsler, V., Dunkel, J., Blayney, M. & Goldstein, R. E. Rheotaxis facilitates upstream navigation of mammalian sperm cells. *Elife* **3**, e02403 (2014).
- [256] Altman, E., Sieberer, L. M., Chen, L., Diehl, S. & Toner, J. Two-dimensional superfluidity of exciton polaritons requires strong anisotropy. *Physical Review X* **5**, 011017 (2015).
- [257] Alicea, J., Balents, L., Fisher, M. P., Paramakanti, A. & Radzihovsky, L. Transition to zero resistance in a two-dimensional electron gas driven with microwaves. *Physical Review B* **71**, 235322 (2005).
- [258] Wachtel, G., Sieberer, L., Diehl, S. & Altman, E. Electrodynamical duality and vortex unbinding in driven-dissipative condensates. *Physical Review B* **94**, 104520 (2016).